Mapping and Monitoring Bluff Erosion with Boat-based LIDAR and the Development of a

Sediment Budget and Erosion Model for the

Elwha and Dungeness Littoral Cells, Clallam County, Washington

GEORGE M. KAMINSKY

HEATHER M. BARON

AMANDA HACKING

DIANA McCANDLESS

Washington State Department of Ecology

Coastal Monitoring & Analysis Program

DAVID S. PARKS

Washington State Department of Natural Resources

ABSTRACT

The spatial distribution and temporal variability of retreat rates of coastal bluffs composed of unconsolidated glacial deposits are of intense interest to landowners who occupy bluff-top properties as well as coastal resource managers who are responsible for protecting marine habitats such as forage fish spawning beaches dependent on bluff-derived sediments. Assessment of the bluff retreat and associated sediment volumes contributed to the nearshore over time is the first step toward development of a coastal sediment budget for bluff-backed beaches. This project develops and applies a boat-based LiDAR system for mapping and monitoring bluff erosion patterns from June 2012 to August 2013 to augment traditional data sources including aerial photography (1939 and 2001), GPS-based beach profile data (2010-2013), and airborne LiDAR (2001 and 2012). These data are analyzed in context to determine alongshore rates of bluff retreat and associated volume change for the Elwha and Dungeness littoral cells in Clallam County, Washington. Recession rates from 2001-2012 range from 0-1.88 m/yr in both drift cells, with mean values of 0.26 ± 0.23 m/yr (N = 152) in Elwha and 0.36 ± 0.24 m/yr (N = 433) in Dungeness. Armored sections show bluff recession rates reduced by 50% in Elwha and 80% in Dungeness, relative to their respective unarmored sections. Dungeness bluffs are estimated to produce twice as much sediment per alongshore distance as the Elwha bluffs (avg. 7.5 m^3/m/yr vs. 4.1 m^3/m/yr, respectively). Historical bluff recession rates (1939-2001) were comparable to those from 2001-2012, but recent annual retreat rates (2012-2013) showed great variation of up to 4.86 m/yr. Rates derived from short time-scales should not be used directly for predicting decadal-scale bluff recession rates for management purposes, as they tend to represent short-term localized events rather than long-term sustained bluff retreat. Analysis with a simple bluff erosion model suggests that predicted rates of sea-level rise have the potential to increase bluff erosion rates by up to 0.1 m/yr by the year 2050.

INTRODUCTION

Coastal bluffs are a dominant geomorphic feature of shorelines of the Strait of Juan de Fuca, Washington State, USA, and are the primary source of sediment contributed to mixed sand and gravel beaches in the region (Schwartz et al., 1987; Shipman, 2004; Finlayson, 2006; Johannessen and MacLennan, 2007). The spatial and temporal distribution of bluff recession from wave-, wind-, precipitation-, and groundwater-induced erosion is poorly understood and documented for the southern shore of the Strait of Juan de Fuca and has led to underestimating the potential hazards to infrastructure (e.g., roads, houses) posed by eroding bluffs over time (Figure 1). Efforts to protect infrastructure and limit the rates of bluff erosion by constructing shoreline revetments have historically ignored the physical and ecological effects of sediment starvation of beaches caused by shoreline hardening (Shipman et al., 2010). The disruption of sediment movement from bluffs to beaches has caused the loss of suitable habitats for critical marine species, including forage fish and juvenile salmonids (Rice, 2006; Shipman et al., 2010; Shaffer et al., 2012; Parks et al., 2013). The importance of understanding the long-term littoral sediment budget has been underscored by the recent removal of two dams on the Elwha River and subsequent introduction of 2.5 x10^6 m^3 of sediment into the nearshore environment within the first two years (between September 2011 and September 2013) (Gelfenbaum et al., in review).

Relatively few studies of coastal bluff recession have been completed for shoreline areas of the Strait of Juan de Fuca, and the studies that have been completed have used a variety of methods leading to difficulty in comparing results. In the Elwha littoral cell (herein referred to as 'drift cell'), the U.S. Army Corps of Engineers (USACE) completed an evaluation of bluff recession rates and sediment volume supply to the nearshore environment as part of an environmental assessment for a shoreline armoring and beach nourishment project on Ediz Hook in Port Angeles (USACE, 1971). The USACE study, using Government Land Office and National Geodetic Survey shoreline maps, estimated a gradual reduction in bluff recession rates from 1.5 m/yr (1850–1885) to 1.3 m/yr (1885–1926), decreasing to 1.1 m/yr (1926–1948), and then to 0.2 m/yr (1948–1970). Each successive reduction in bluff recession rates since 1930 has been attributed to construction and maintenance of a multitude of shoreline armoring projects at the base of the Elwha bluffs (USACE, 1971).

The USACE (1971) study also shows a reduction in sediment volumes provided by the Elwha bluffs over time. Prior to the Elwha Dam construction, the estimated sediment supply from the bluffs was 2.22 x 10^5 m^3/yr. After construction of the Elwha Dam in 1911 and prior to construction of shoreline armoring along the Elwha bluffs in 1930, the estimated sediment supply from the bluffs was nearly the same at 2.06 x 10^5 m^3/yr. Between 1930 and 1961 when substantial shoreline armoring along the bluffs was installed and maintained, the bluff sediment supply decreased to 0.73 x 10^5 m^3/yr. Following the completion of a major shoreline armoring project along the bluffs in 1961, bluff sediment supply was estimated to have further declined to 0.306 x 10^5 m^3/yr. The reduction of bluff-supplied sediment over this entire time period, 1.91 x10^5 m^3/yr, represents an 85% reduction in the coastal sediment supply to Ediz Hook (Galster, 1989), which is essentially equivalent to the pre-dam fluvial sediment supply estimated by Randle et al. (1996).

Bluff erosion rates to the east of the Dungeness drift cell along the Strait of Juan de Fuca were evaluated through land-parcel surveys by Keuler (1988). Bluff recession rates up to 0.30 m/yr and sediment production rates of 1-5 m^3/m/yr were observed in areas exposed to wave attack associated with long fetches. On the west side of Whidbey Island, at the eastern limit of the Strait of Juan de Fuca, Rogers et al. (2012) determined long-term bluff erosion rates of 0-0.08 m/yr using cosmogenic [10]Be concentrations in lag boulders to date shoreline positions over time scales of 10^3-10^4 years.

Though these techniques aim to provide estimates of bluff recession rates and sediment supply volume, a more robust way to quantify bluff sediment supply to the beach is to compare accurate digital elevation model (DEM) surfaces from before and immediately after a bluff failure. Traditional methods for analyzing bluff change such as delineation of bluff edges on aerial photographs are subject to large uncertainties and cannot quantify change at this detail. Airborne LiDAR produces poor coverage on vertical surfaces. Terrestrial LiDAR is the newest and most accurate technology being used to map and monitor coastal bluff change (e.g., Quan et al., 2013; Olsen et al., 2008, 2009; Young and Ashford, 2007; Young et al., 2009; Alho et al., 2009; Buckley et al., 2008; Collins and Sitar, 2005, 2008; Stewart et al., 2009). In particular, boat-based LiDAR offers a promising method for measuring coastal bluff change along the Washington coast.

Boat-based LiDAR can be mobilized quickly and produce high-resolution images that detect small changes in bluffs, including wave cut notches (Storlazzi et al., 2007). It enables remote monitoring of areas otherwise difficult to survey by traditional methods due to private property, personal hazard, loss of GPS satellite and radio signal due to proximity to bluffs, or other logistical issues. Furthermore, boat-based LiDAR is shown to be nearly four times more accurate vertically than airborne LiDAR (Stewart et al., 2009) and significantly less expensive at the project scale.

In this study we derive estimates of short- and long-term bluff recession rates and associated sediment volumes contributed to the Elwha and Dungeness drift cells along the Central Strait of Juan de Fuca between 1939 and 2013 from a variety of sources, including historical aerial photography, GPS beach profiles, airborne LiDAR, and newly collected boat-based LiDAR, implemented specifically for this project. We evaluate the relative importance of bluff-derived sediment supply to the nearshore in the context of a coastal sediment budget recently rejuvenated by the removal of two dams on the Elwha River. We use the documented rates of bluff recession for the Elwha and Dungeness drift cells in the application of a simple bluff recession model, following an approach by Lee (2005), to provide estimates of potential future coastal bluff recession under varying rates of sea-level rise (Mote et al., 2008). Finally, we evaluate the use of boat-based LiDAR in monitoring coastal bluffs, comparing the data we collect with existing airborne LiDAR.

Figure 1. A) Bluff-top homes threatened by receding bluffs, Dungeness drift cell. B) Seawall installed at bluff toe to protect Port Angeles City Landfill from bluff retreat, Elwha drift cell.

STUDY AREA

The study area is located on the southern shore of the Central Strait of Juan de Fuca near the city of Port Angeles, Washington (Figure 2). The study area is divided into two distinct shoreline segments which encompass separate but adjacent littoral cells with bluff-backed beaches: the Elwha bluffs extend along the central portion of the Elwha drift cell and the Dungeness bluffs extend along the western portion of the Dungeness drift cell (Figure 3). Each drift cell contains an updrift segment of eroding coastal bluffs to the west that supply sediment via longshore littoral transport to long spits at the down-drift end to the east.

The Elwha bluff segment is 4.9 km long and supplies sediment to Ediz Hook. The Dungeness bluff segment is 13.6 km long and supplies sediment to Dungeness Spit. A fundamental difference between the two drift cells is that the Elwha River discharges into the Strait of Juan de Fuca updrift of the Elwha bluffs, while the Dungeness River empties into the Strait of Juan de Fuca on the lee side of Dungeness Spit (Figure 2). Therefore, the Elwha drift cell is composed of both river- and bluff-derived sediments, while the Dungeness drift cell is composed of only bluff-derived sediments.

The Strait of Juan de Fuca is a wind-dominated marine system which exhibits net easterly longshore sediment transport within the intertidal zone of the study area (Schwartz et al., 1989; Galster and Schwartz, 1989; Warrick et al., 2009; Miller et al., 2011). Winds in the Central Strait of Juan de Fuca are dominantly west and northwesterly with a minor component of north and northeasterly winds (Miller et al., 2011). Therefore, both the Elwha and Dungeness drift cells exhibit net easterly littoral sediment transport (USACE, 1971; Schwartz et al., 1989; Galster and Schwartz, 1989).

The wave climate of the Central Strait of Juan de Fuca is similarly dominated by west to northwest wind waves and west to northwest swells from the Pacific Ocean. Maximum wave heights within the study area range up to 3 m whereas average heights are 0.5 m (USACE, 1971; Gelfenbaum et al., 2009; Warrick et al., 2009; Miller et al., 2011). Gelfenbaum et al. (2009) has modeled the distribution of significant wave heights within the Central Strait of Juan de Fuca, and given a 2 m swell at the entrance to the Strait of Juan de Fuca, nearshore wave heights of 1 m are shown throughout the study area, but with significant alongshore variability in wave height due to wave focusing or sheltering, and in wave direction due to refraction.

Tides within the Strait of Juan de Fuca are mixed-diurnal with two high and low tides per day. Tidal elevations range between -1.0 m and +3.7 m elevation (NAVD 88) (Zilkoski et al., 1992; NOAA, 2013).

A precipitation gradient exists from west to east within the study area due to a rain-shadow effect of the Olympic Mountains. Average annual precipitation (1971-2000) in the Elwha drift cell is 10.1 cm vs. 6.3 cm in the Dungeness drift cell (Drost, 1986; NCDC, 2014). Maximum rainfall intensities within the Elwha drift cell are 1.4 cm/hr, vs. 1.1 cm/hr in the Dungeness (Drost, 1986; NCDC, 2014). Precipitation occurs primarily as rain, with the wettest months between October and April, and a seasonal dry period between May and September. Freezing temperatures occur

within the study area between October and May, and snowfall intermittently occurs in the period between November and April.

Groundwater recharge occurs along the Olympic Mountains and discharges into the Strait of Juan de Fuca. Local groundwater recharge occurs within low-elevation glacial landforms adjacent to the coastal bluffs and discharges at varying elevations on the bluffs controlled by local aquitards (i.e., beds of low permeability materials composed of dense silt, clay and till) (Drost, 1986; Jones, 1996).

The surficial geology of the study area is dominantly composed of Pleistocene continental glacial deposits overlying pre-Fraser non-glacial sediments associated with an Elwha River source (Schasse et al., 2000; Polenz et al., 2004) and Eocene marine sedimentary rocks (Schasse et al., 2000; Schasse and Polenz, 2002, Schasse, 2003; Polenz et al., 2004). Pleistocene glacial deposits occurring within the study area include recessional outwash, glaciomarine drift, and glacial till.

The shoreline within the study area exhibits steeply sloping to vertical and overhanging coastal bluffs up to 80 m high created by changes in relative sea level from post-glacial rebound following Cordilleran glacial retreat; erosion of the shoreline in the study area began around 5400 years before present (Downing, 1983; Dethier et al., 1995; Booth et al., 2003; Schasse, 2003; Polenz et al., 2004; Mosher and Hewitt, 2004).

Bluff recession within the study area is dominated by shallow landsliding in the form of topples, debris avalanches, flows and slides (Varnes, 1978). Other types of gravitational failures are also present, including stress release fracturing (Bradley, 1963), cantilever, and Culmann-type failures (Carson and Kirkby, 1972). These types of shallow mass wasting processes are common in sea cliffs composed of weakly lithified sediments (Hampton, 2002). Aeolian erosion during dry periods in the form of ravel is also observed. Aerial, boat, and ground-based surveys of the study area have determined the absence of deep-seated (Varnes, 1978) landslides consistent with existing geologic mapping (Schasse et al., 2000; Schasse and Polenz, 2002; Schasse, 2003; Polenz et al., 2004). Processes driving shallow landsliding include over-steepening and subsequent failure of bluffs from wave-induced erosion at the bluff-base and the development of high pore-water pressures within hillslopes during storms.

Land-use above the bluffs varies throughout the study area from dense urban development in the Elwha drift cell within the City of Port Angeles, to native second-growth forest within the Dungeness drift cell. Vegetation within the study area ranges from dense stands of mature second- and third- growth Douglas fir forest to open grass associated with urban lawn-scapes.

The sediment budget of the Elwha drift cell has substantially declined as a result of human-induced changes. The construction of coastal revetments began in the Elwha drift cell shortly after the construction of two dams on the Elwha River in the early 20th century (Galster, 1989). In 1929, a coastal revetment was installed between Dry Creek and Ediz Hook to protect an industrial waterline that supplied water from the Elwha River to paper mills on Ediz Hook. Within six years of the placement of coastal defense works, Ediz Hook began to erode due to the reduction in sediment supply from bluffs (Galster, 1989). Galster (1989) estimated that in the Elwha drift cell, 15% of the sediment supplying Ediz Hook originated from the Elwha River and

85% was supplied from coastal bluff erosion prior to construction of Elwha River dams and coastal revetments. Galster (1989) estimated that coastal armoring in the Elwha drift cell resulted in an 89% reduction of sediment volume supplied to Ediz Hook. In 1975, the USACE and the City of Port Angeles armored the shoreline of Ediz Hook and began a program of beach nourishment that continues to the current time. In 2005, the City of Port Angeles constructed a 400 foot-long concrete, steel, and rock seawall at the Port Angeles Landfill. Currently 68% of the Elwha bluffs are armored with rip-rap or constructed seawalls. In contrast, less than 1% of the length of the Dungeness bluffs is armored.

In 2012, the Elwha Dam on the Elwha River was completely removed and, as of 2014, the Glines Canyon Dam has been almost completely removed, resulting in the delivery of 2.5×10^6 m^3 of predominantly fine sediment to the nearshore of the Elwha littoral cell within the first two years since dam removal began in September 2011 (Gelfenbaum et al., in review). This sediment volume represents approximately 12% of the total sediment stored in both reservoirs. It is estimated that within 7-10 years following the complete removal of both Elwha River dams, the long-term annual sediment contribution from the Elwha River to the nearshore will be approximately 0.25×10^6 m^3/yr (Gilbert and Link, 1995; Bountry et al., 2010).

Understanding the relative contribution of bluff erosion to the overall sediment budget of the Elwha drift cell will help with efforts to manage the long-term coastal environment once the reservoir sediments released by dam removal have been transported out of the fluvial network and into the Strait of Juan de Fuca.
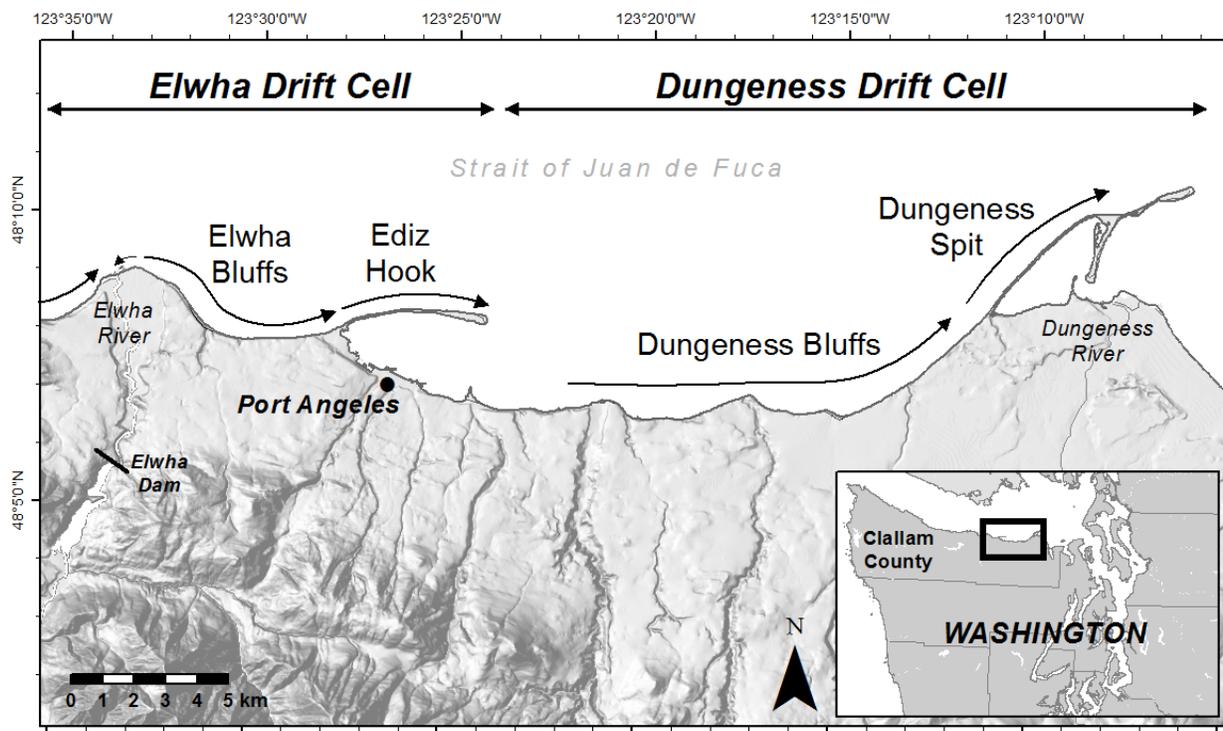
Figure 2. Map of the study area showing direction of net alongshore sediment transport within the Elwha and Dungeness drift cells in Clallam County, Washington.

Figure 3. A) Photograph of the Dungeness bluffs looking west from Dungeness Spit. B) Photograph of the Elwha bluffs west from Ediz Hook. Note the armoring placed mid-beach in front of the bluffs.

METHODS

Bluff-Face Change Mapping

Short- and long-term coastal bluff recession rates for the Elwha and Dungeness drift cells were determined by analyzing data from several sources, including historical aerial photographs, existing airborne LiDAR data, and newly collected boat-based LiDAR data. In order to make comparisons of the bluffs between the three data types, two-dimensional cross-shore transects were established in each drift cell at 100-ft (30-m) intervals, except where interrupted by coastal streams or ravines (Figure 4). The transects extend across the beach and up the bluff face, to at least the bluff crest (as was the case for the boat-based LiDAR set), along which retreat distances could be calculated. Bluff retreat was measured between consecutive surveys at the bluff crest for aerial photos and at selected elevations across the bluff face for LiDAR data.

Long-term bluff change
Bluff recession rates for 1939-2001 were determined by calculating the distance between bluff crest positions on georeferenced historical aerial photographs. Prior to analysis, aerial photographs were scanned, georeferenced, and imported into ArcGIS v. 10.1 (ESRI, Redlands, CA) and bluff crest positions were digitized for study segment areas unobstructed by vegetation. Distances between the 1939 and 2001 bluff crest positions were measured at each transect location.

Recession rates for 2001-2012 were determined from the differences in horizontal position of selected elevations on bluff-face profiles extracted from digital elevation models (DEMs) available from recent airborne LiDAR datasets, using methods outlined in Hapke (2004) and Young et al. (2010, 2011). For this analysis, we used a 2001 bare earth DEM (2-m grid) from the Puget Sound LiDAR Consortium (PSLC, 2001) that covered the entire survey area, 2012 Clallam County LiDAR (1-m grid; Yotter-Brown and Faux, 2012) for the Dungeness drift cell, and 2012 LiDAR data (0.5-m grid) from the U.S. Geological Survey (USGS, 2012) for the Elwha drift cell. DEMs were imported into ArcGIS and evaluated using the 3D Analyst toolset. At each transect location a two-dimensional topographic profile from the mid beach to the bluff-crest was extracted from each DEM. The net horizontal distance between the two profiles was measured at 6-m vertical intervals between the bottom and top of the bluff face. The difference in total cross-sectional area between the 2001 and 2012 topographic profiles was measured and multiplied by a unit width to estimate a volume of sediment lost between the two DEMs.

Statistical evaluation of the data for bluff recession and sediment volume contributions from the airborne LiDAR DEMs was performed using exploratory data analysis methods (EDA) (Schuenemeyer and Drew, 2011). Bluff recession distance values were tested for spatial trend and normalized using a lognormal transformation. Summary statistics were then computed using the de-trended values. Sources of error include internal error in the LiDAR data acquisition and processing technique, as well as differences in grid size of the LiDAR-derived DEMs.

Short-term bluff change
To assess short-term bluff recession rates and take advantage of a new technique, boat-based LiDAR was collected along both the Dungeness and Elwha drift cells on three occasions during

2012-2013 by the Washington State Department of Ecology, Coastal Monitoring & Analysis Program (CMAP), aboard the R/V *George Davidson*. Data from the most recent survey conducted August 2013 was compared to the most recent airborne LiDAR data (2012 Clallam County LiDAR for the Dungeness drift cell and 2012 USGS LiDAR for the Elwha drift cell) to determine bluff recession rates and sediment volume contributions between 2012 and 2013 along the pre-defined transects. Data from all three boat-based LiDAR datasets was examined from a three-dimensional perspective (comparing surfaces rather than transects) for a select portion of the Dungeness drift cell to more closely examine bluff erosion patterns and evaluate the use of the technology for future monitoring.

During data acquisition, the research vessel was equipped with an Optech ILRIS-HD-ER laser scanner with motion compensation and an Applanix Position and Orientation System for Marine Vessels (POS MV 320 V5 RTK), consisting of an inertial measurement unit (IMU), two GNSS antennas, and a computer system, which supplies the acquisition computer with accurate timing for synchronization of LiDAR data along with real-time position and orientation of the vessel. Data from the IMU and laser scanner are integrated with QINSy v. 8.10 (Quality Positioning Services, Zeist, The Netherlands), a navigation and hydrographic survey software which allows the operator to monitor the incoming point cloud data, corrected for the motion of the vessel, in real-time. When scanning from a mobile platform, the laser is set to scan in a vertical line with a maximum fixed interval such that at a scan distance of 100-200 m, the vertical spacing of the returns are ~15-30 cm. The data density alongshore is controlled by the speed of the vessel; therefore, both the computer operator and boat operator work closely together, communicating constantly about data gaps and density patterns so that the boat operator can maneuver the boat forward and aft to sweep the laser across the landscape.

High-resolution digital photographs were simultaneously taken of the shoreline with approximately 40% overlap between frames and from multiple perspectives. Photomosaics were generated by stitching together overlapping photos using Autopano Giga Pro v. 3.0.3 (Kolor, France) which accounts for the moving reference point of the vessel. These photomosaics were used while cleaning the laser point cloud to help discern questionable data from true returns and identify vegetation or anomalous features.

During the boat-based LiDAR surveys, high-contrast targets were placed along the shoreline throughout the study area as ground control points (Figures 5 and 6). The targets were surveyed using a Trimble R8-3 GNSS rover (Figure 6) receiving real-time corrections via the internet from the Washington State Virtual Reference Network (30-s occupation). The target positions are used to check the accuracy of the georeferenced point cloud. The on-ground survey crew also took control points on various Washington State Department of Transportation (WSDOT) benchmarks located near the survey area.
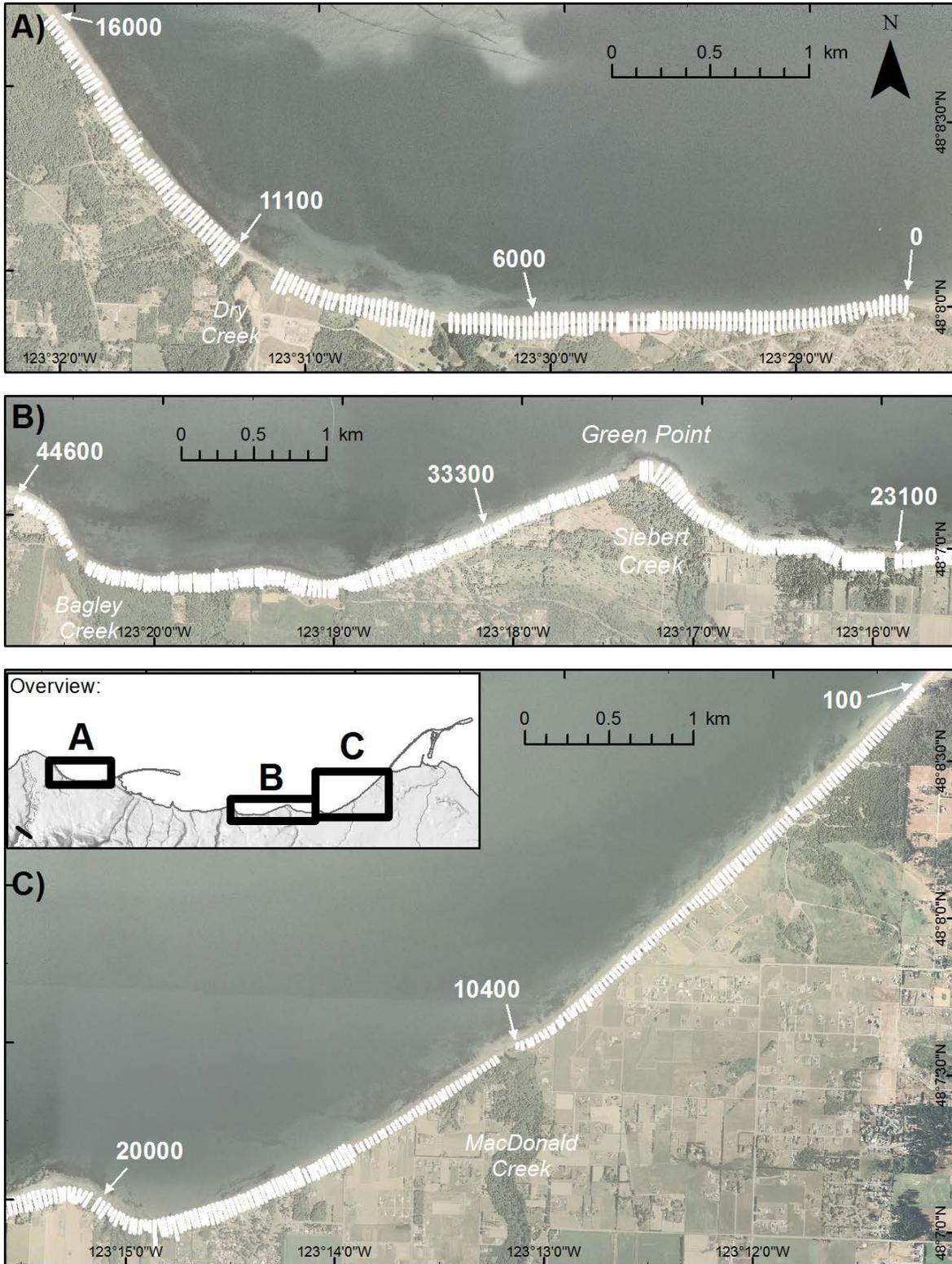
Figure 4. Map showing transect locations for the Elwha bluffs (A) and Dungeness bluffs (B = west, C = east).
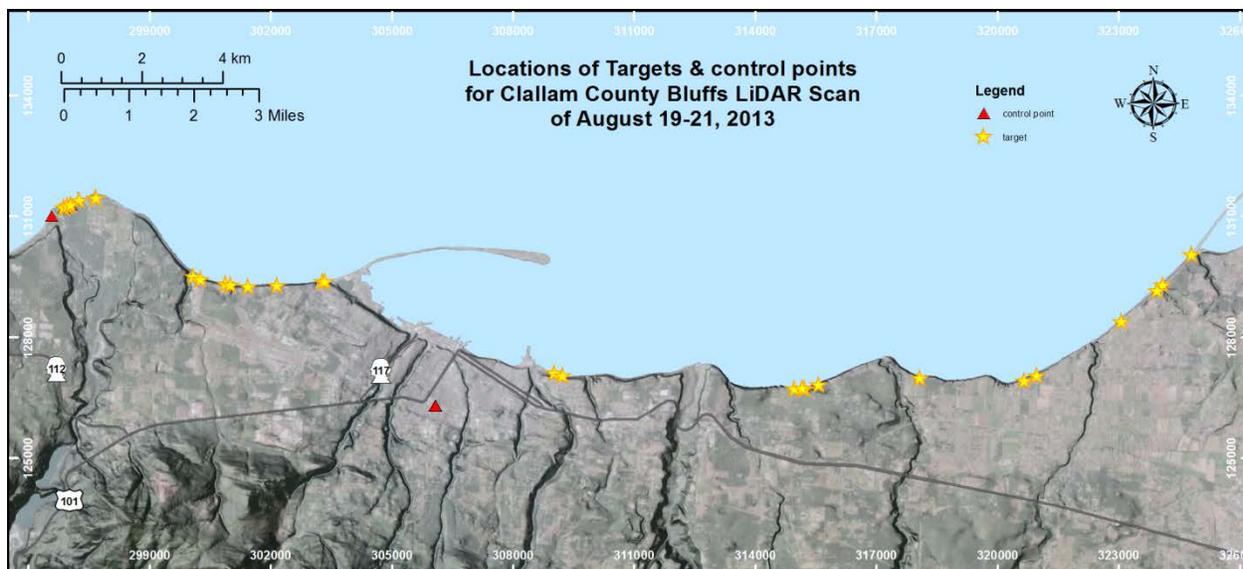
Figure 5. Map of study area showing locations of targets setup for ground control during the third boat-based LiDAR survey in August 2013, as well as benchmarks surveyed as control points.

Figure 6. A) Photo showing a plywood target setup for ground control during the boat-based LiDAR survey. B) Photo showing the use of a Trimble R8 GNSS receiver to obtain the position of a ground control target.

The vessel position (XYZ) for the third boat-based LiDAR dataset (August 2013) was post-processed in POSPac MMS v 6.2 (Applanix, Ontario, Canada) using a SmartBase network of six reference stations to generate a smoothed best estimate of trajectory (SBET) which was applied to the point cloud data in QINSy. The data was cleaned in Qloud v. 2.3 (Quality Positioning

Services, Zeist, The Netherlands) to remove high fliers and noise resulting from reflections in the water surface or sun glare. Next, the point cloud was classified in VG4D (Virtual Geomatics, Austin, TX) to remove vegetation and retain only the ground surface, using the photomosaics for reference. The ground feature class was then imported into ArcGIS and transects were extracted using a 1-m node spacing and linear interpolation for comparison with the 2012 airborne LiDAR datasets.

The first and second boat-based LiDAR datasets (from June 2012 and March 2013) were cleaned using the 3D Editor in Fledermaus v. 7.4 (Quality Positioning Services, Zeist, The Netherlands) to remove reflections in the water surface, sun glare, and vegetation above the top of the bluff. After assessing the data density, the point clouds for all three datasets were gridded in DMagic, a Fledermaus application, using a bin size of 0.8 m. A three-dimensional vector shift was applied to the DEMs for the first and second surveys in MATLAB R2013b (MathWorks, Natick, MA) to align them with the third, georeferenced DEM using a number of fixed points along the shore (i.e., large boulders).

To quantify volume change between the three boat-based LiDAR DEMs, difference surfaces were produced by subtracting one surface from another in Fledermaus (e.g., the second dataset from the first dataset). These difference surfaces can be color-coded to show positive or negative differences, indicating where accretion or erosion has occurred along the beach and bluff between the two surveys, as a way to visualize volume change.

Beach Profile Change Monitoring

To assess general trends in beach elevation change (m/yr) and estimate rates of sediment flux on the beaches (m^3/m/yr), two-dimensional, cross-shore topographic beach profiles at 12 locations, eight along the Dungeness bluffs and four along the Elwha bluffs, were surveyed between 2010 and 2013 with a ProMark 800 and 200 Real-Time Kinematic Global Positioning System (RTK-GPS). Elwha and Dungeness drift cell beach profiles were collected in all seasons. Profiles were oriented normal to the slope of the beach, extending from the base of coastal bluffs to the low water limit. Elevation measurements were recorded along each transect at horizontal intervals of approximately 5 ft (1.5 m). RTK-GPS measurement accuracy ranged from 1-5 cm based on repeat measurements of fixed control points across the study area.

Sediment volume changes were calculated using the upper 20 m of each profile, which was the extent of overlap between all surveys. The elevation difference between each pair of profiles was calculated every 0.5 m, with a linear interpolation between the original 1.5 m data point spacing. The difference values along the entire transect were averaged to yield a single value of average elevation change per transect. The average elevation change was multiplied by the 20-m length of the profile and an alongshore unit width of 1 m to yield a volume change per alongshore meter (m^3/m) for the 20 m of upland beach.

Bluff Recession Model

To provide the upper and lower bounds of anticipated future bluff recession, we apply a simple model of bluff recession (Lee, 2005) using future potential scenarios of sea-level rise and beach morphology change to estimate future rates of recession from those observed in this study. The model proposed by Lee (2005) uses a modification of the Bruun Rule (Dean, 1991; Bray and Hooke, 1997) to calculate future bluff recession rates, R, as follows:

$$R = R_1 + Sc\frac{L}{P(B + H)}$$

where R_1 is the historical recession rate (m/yr), Sc is the change in rate of sea-level rise (m/yr), P is the sediment overfill (the proportion of sediment retained in the equilibrium beach profile), B is the cliff height (m), H is the closure depth (m)—the depth at the seaward-most extent beyond which there is no significant change in bottom elevation and no significant net sediment transport between the nearshore and the offshore over an annual time scale (Kraus et al., 1998), and L is the total horizontal distance between the bluff top and the closure depth (Figure 7).

This study calculated R_1 and B as previously described. Values for Sc and P were taken from previously published studies (Mote et al., 2008; Parks et al., 2013). The closure depth was calculated from seasonal bathymetric profiles collected by the USGS (Andrew Stevens, 2014) in the Elwha drift cell in September of 2004, 2005, and 2013, and May of 2013 and 2014 using personal watercraft equipped with single-beam sonar systems. Transects were oriented perpendicular to the shoreline and extended from mid-beach to at least -10 m NAVD 88.

Analysis of the bathymetric profiles was conducted in Matlab R2013b (MathWorks, Inc., Natick, MA). Little change was observed from survey to survey in these profiles, so the major nearshore inflection point of the profile was chosen as a proxy for the point of insignificant annual profile change (i.e., closure depth). In order to detect and select the inflection point at each transect, an average profile was calculated to smooth noise from the data, using a moving average window of +/- 50 m. The shoreface slope was calculated from the average profile by comparing depth values at +/- 25 m across-shore from each query point. Concavity (i.e., rate of change in slope) was then calculated by sampling the slope at +/- 50 m. The concavity varied across and along profiles, sometimes with several points of inflection visible in the data. The point of major change from concave up to concave down was visually selected using best judgment and with the context of neighboring profiles to determine the location of the closure depth. This morphological feature is essentially defined at the point at which the upper shoreface slope ceases to change significantly and a significant concavity inflection exists at the base of the upper shoreface, often at the transition to a concave-downward lower shoreface.

The Dungeness drift cell lacks detailed bathymetry data required to perform a similar analysis of the closure depth based on morphology. An average distance was determined from the most resolvable nearshore break in slope in order to obtain input for the erosion model from 30-ft (10-m) gridded bathymetry (Finlayson, 2005).

$$R = R_1 + S_c \frac{L}{P(B+H)}$$

R = future recession rate

R$_1$ = past recession rate

Bluff Top

B = bluff height

P = sediment overfill %

S$_c$ = sea level rise

Bluff Toe

H = closure depth

Depth of Closure

L = length of bluff/beach profile
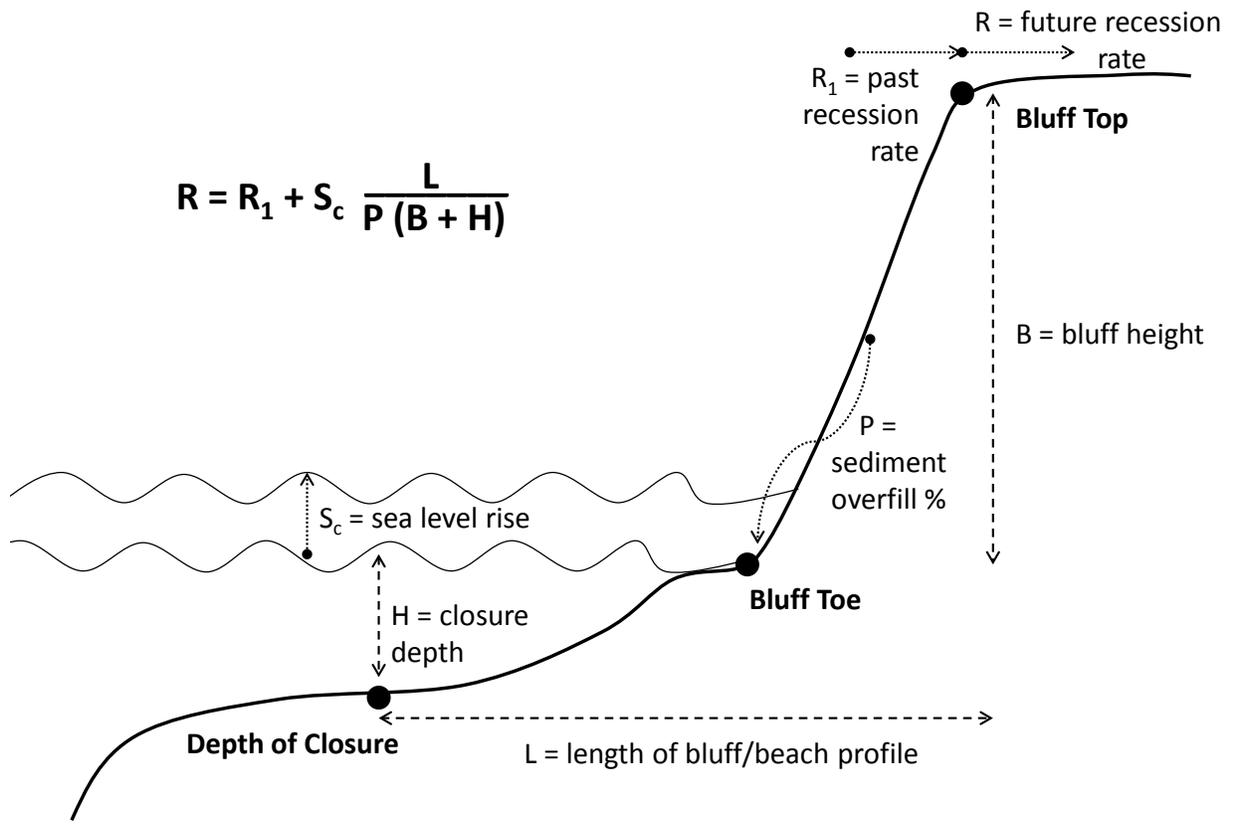
Modified Bruun Rule (Lee, 2005)

Figure 7. Diagram showing the bluff erosion model parameters used by Lee (2005) and applied herein.

RESULTS

Bluff-Face Change

Long-term bluff change
Observed rates of coastal bluff recession are highly variable across both drift cells (Figures 8-10). Table 1 provides data results from sections of each drift cell with unobstructed views of the bluff edge in aerial photography from 1939 and 2001, and includes identical shoreline reaches used for a comparison of rates derived from airborne LiDAR from 2001 and 2012. The data show a recent decrease in mean recession rate in the Elwha drift cell (-0.22 m/yr), and a slight increase in mean recession rate in recent years in the Dungeness drift cell (+0.1 m/yr).

Table 1. Recession rates (m/yr) from aerial photography (1939-2001) and airborne LiDAR (2001-2012) for unobstructed bluff-edge reaches of each drift cell.

Drift Cell	Period	Min. (m/yr)	Mean (m/yr)	Max. (m/yr)	S.D. (m/yr)	N (# transects)	Length (m)
Dungeness	1939-2001	0.0	0.40	1.00	0.20	181	5639
	2001-2012	0.1	0.50	0.90	0.17	181	5639
Elwha	1939-2001	0.2	0.42	0.60	0.10	75	2469
	2001-2012	0.0	0.20	0.55	0.10	75	2469

Table 2 provides data results that extend along the full length of the bluffs in each drift cell. The maximum observed rate of recession between 2001 and 2012 in both drift cells was 1.88 m/yr, associated with the Monterra housing development in the Dungeness drift cell (Figure 1A) and erosional hotspots along the Port Angeles Landfill revetment in the Elwha drift cell (Figure 1B). The mean recession rate in the Dungeness was 0.36 m/yr vs. 0.26 m/yr for the Elwha drift cell (Table 2) for the period 2001-2012.

Table 2. Recession rates (m/yr) by drift cell and shoreline type, 2001-2012.

Drift Cell	Shoreline Type	Min. (m/yr)	Mean (m/yr)	Max. (m/yr)	S.D. (m/yr)	N (# transects)	Length (m)
Dungeness	Unarmored	0.0	0.37	1.88	0.79	423	13,320
	Armored	0.0	0.08	0.46	0.40	10	305
	All	0.0	0.36	1.88	0.24	433	13625
Elwha	Unarmored	0.0	0.40	1.88	1.3	60	1829
	Armored	0.0	0.21	0.58	0.40	92	3048
	All	0.0	0.26	1.88	0.23	152	4877
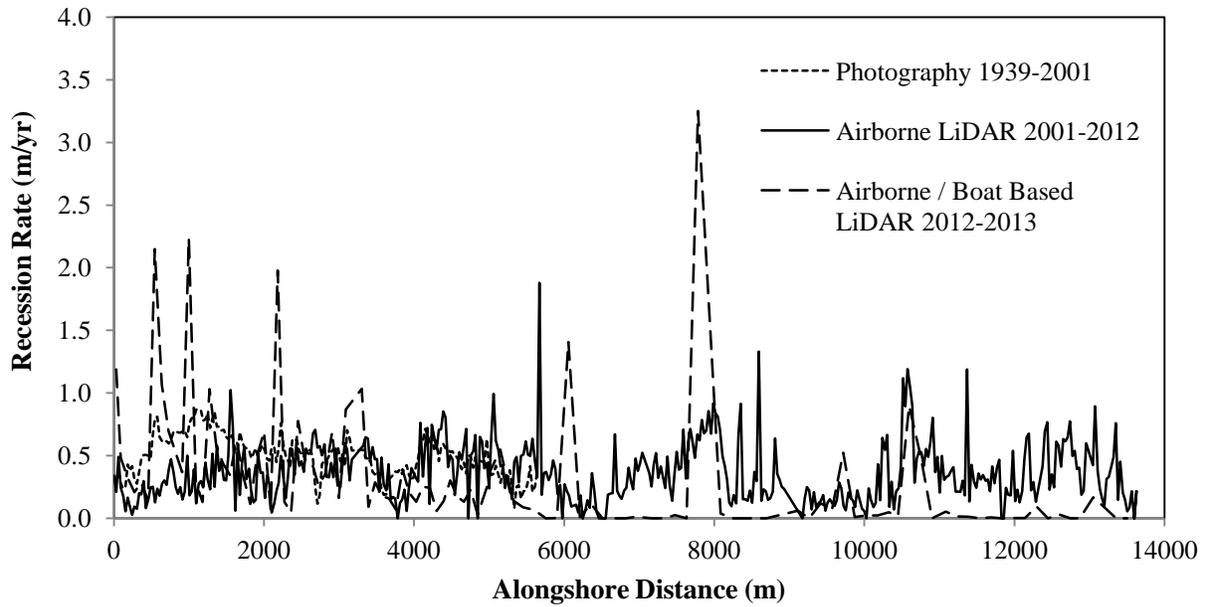
Figure 8. Maximum observed bluff recession rates (m/yr) in the Dungeness drift cell for the time periods 1939-2001 (derived from aerial photography), 2001-2012 (derived from airborne LiDAR), and 2012-2013 (derived from airborne and boat-based LiDAR).
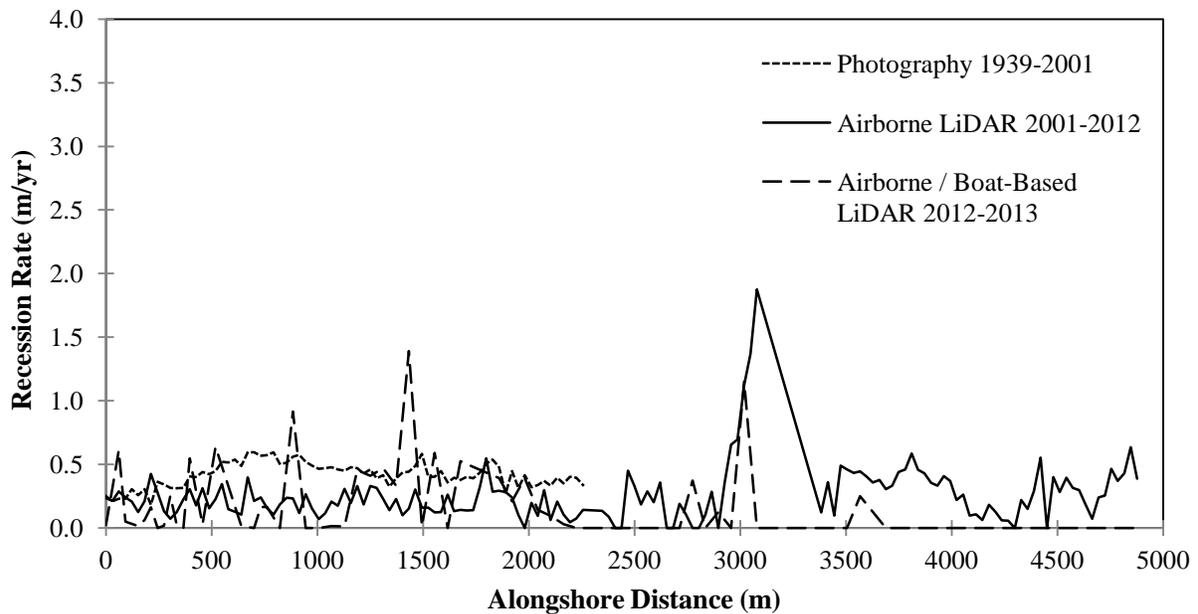
Figure 9. Maximum observed bluff recession rates (m/yr) in the Elwha drift cell for the time periods of 1939-2001 (derived from aerial photography), 2001-2012 (derived from airborne LiDAR), and 2012-2013 (derived from airborne and boat-based LiDAR).

In both drift cells, armored sections of bluffs showed significantly lower rates of recession than unarmored sections: 80% less in the Dungeness drift cell and 50% less in the Elwha drift cell (Table 2; Figure 10). Unarmored bluff sections demonstrated very similar mean rates of recession between drift cells: 0.37 m/yr for Dungeness and 0.40 m/yr for Elwha (Table 2; Figure 10). Unarmored sections of bluffs directly downdrift and adjacent to armored sections experienced the highest rates of bluff recession in the Elwha drift cell (1.88 m/yr) and higher than mean rates (1.0 m/yr) in the Dungeness drift cell (Figure 10).
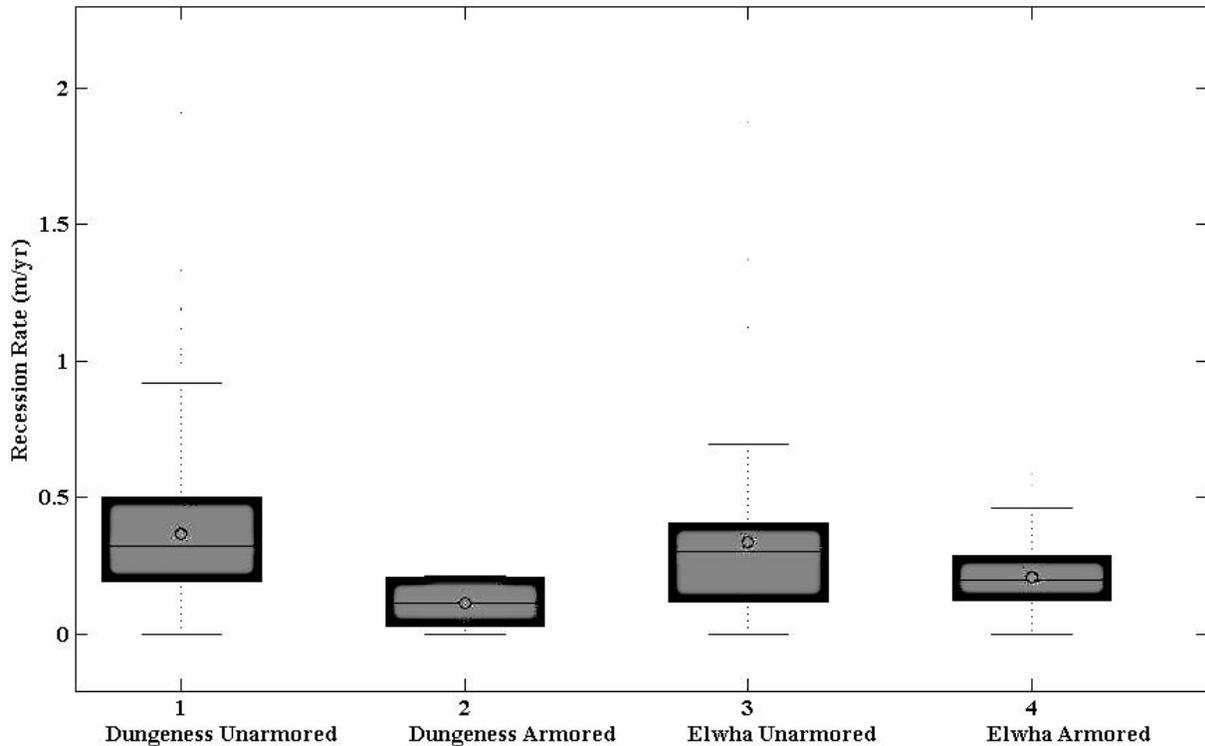
Figure 10. Boxplot of recession rates (m/yr) by drift cell and shoreline type (created in ABOXPLOT; Bikfalvi, 2012). The central line within the box represents the sample median, while the circle represents the sample mean. The upper and lower limits of the box represent the 50th percentile of the population and the whiskers the 75th percentile. Dots beyond the upper and lower whiskers represent outliers of the population.

Sediment volumes eroded from bluffs in the Dungeness drift cell were almost double those observed in the Elwha drift cell per transect (Table 3; Figures 11-13). The mean sediment production rate in the Dungeness drift cell was 25.4 m^3 per transect, vs. 13.8 m^3 per transect in the Elwha drift cell. Rates of sediment production from unarmored sections of bluffs were similar between drift cells. Mean values for sediment production from unarmored sections of bluffs in the Dungeness drift cell were 25.8 m^3 per transect vs. 22.0 m^3 per transect for the Elwha drift cell (Table 3). Sediment production rates for armored sections of bluffs were twice as high in the Elwha drift cell (11.9 m^3 per transect) than the Dungeness drift cell (5.8 m^3 per transect) (Table 3; Figure 13).

Table 3. Sediment volume contribution per transect (m^3) by drift cell and shoreline type, 2001-2012

Drift Cell	Shoreline Type	Min. (m^3)	Mean (m^3)	Max. (m^3)	S.D. (m^3)	N (# transects)	Length (m)
Dungeness	Unarmored	0.0	25.8	163.3	24.3	423	13,320
	Armored	0.0	5.8	9.6	3.8	10	305
	All	0.0	25.4	124.8	31.7	433	13,625
Elwha	Unarmored	0.0	22.0	143.6	30.1	60	1,829
	Armored	0.0	11.9	41.2	7.9	92	3,048
	All	0.0	13.8	159.9	35.9	152	4,877
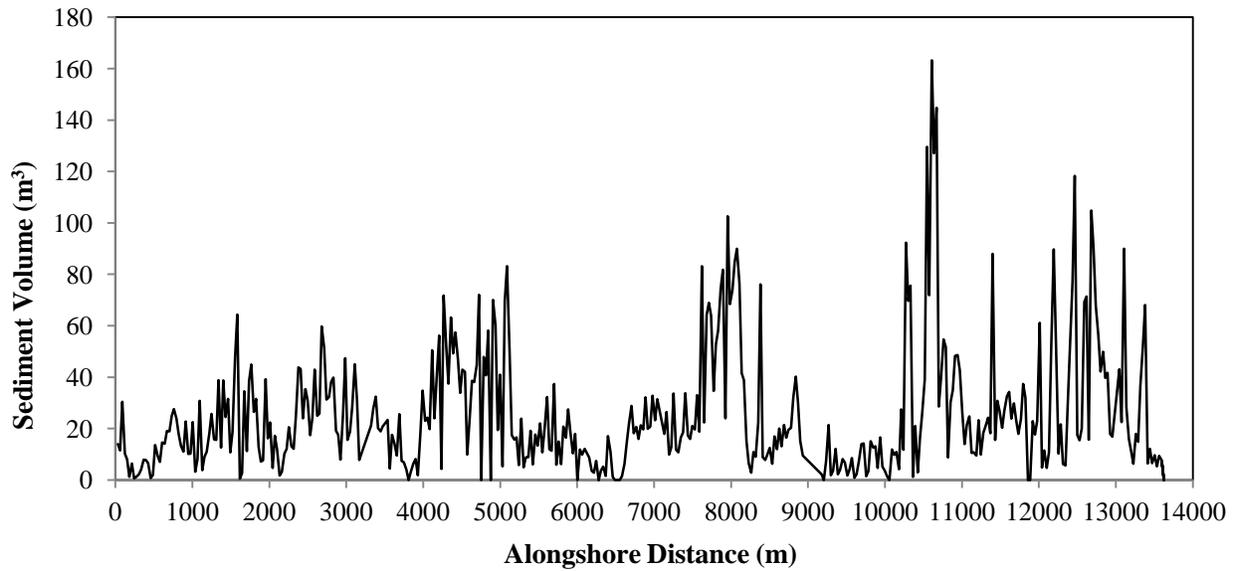
Figure 11. Sediment volume (m^3) per transect in the Dungeness drift cell between 2001-2012.
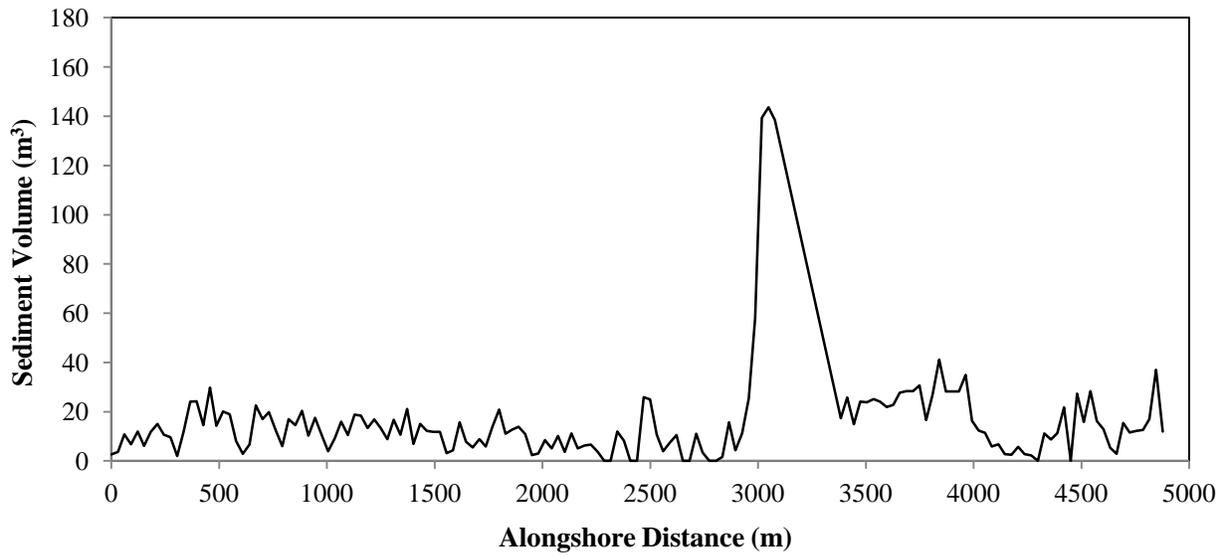
Figure 12. Sediment volume (m^3) per transect in the Elwha drift cell between 2001-2012.
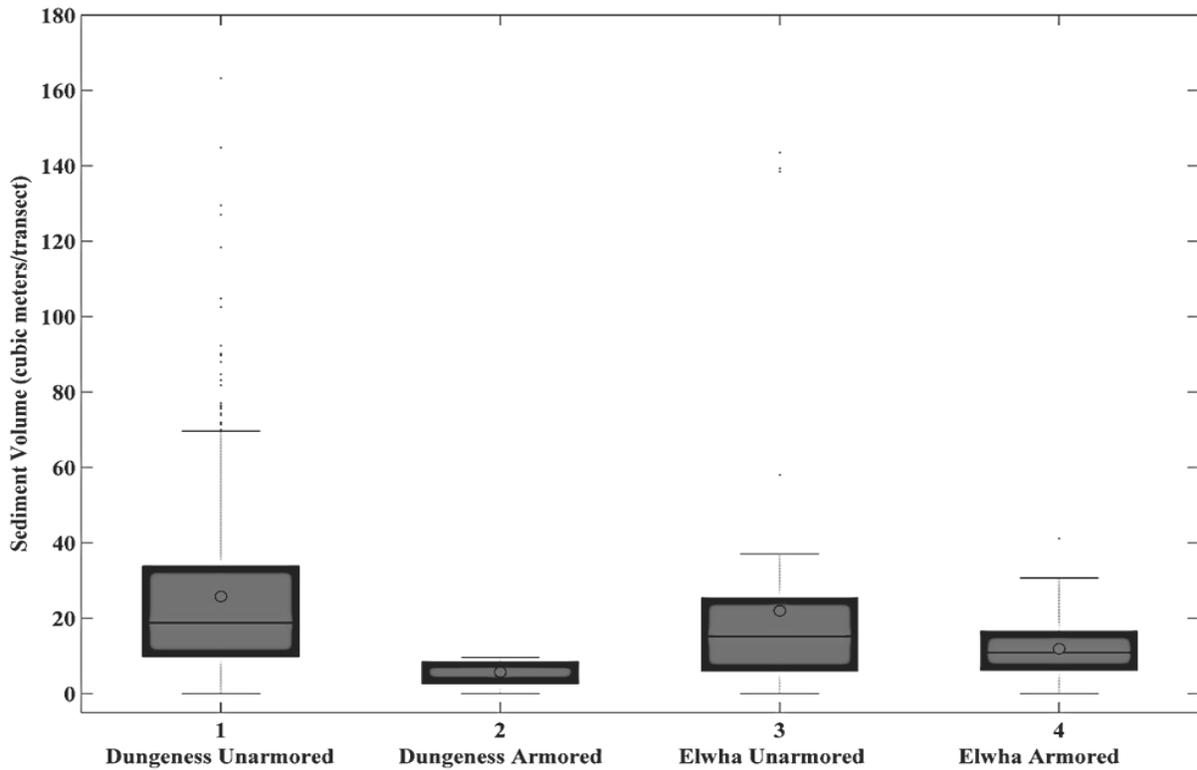
Figure 13. Box plot of sediment volume contributions (m^3/transect) by drift cell and shoreline type (created in ABOXPLOT; Bikfalvi, 2012). The central line within the box represents the sample median, while the circle represents the sample mean. The upper and lower limits of the box represent the 50th

percentile of the population and the whiskers the 75th percentile. Dots beyond the upper and lower whiskers represent outliers of the population.

At the drift cell-scale, the Dungeness bluffs produced approximately five times the volume of sediment of the Elwha bluffs, on average, (1.03×10^5 m^3/yr vs. 0.2×10^5 m^3/yr, respectively) on an annual basis over the 2001-2012 period bluffs (Table 4). When normalized for length, the Dungeness bluffs contributed approximately 55% more sediment than the Elwha bluffs to the nearshore (7.5 m^3/m/yr vs.4.1 m^3/m/yr, respectively) on an annual basis for the 2001-2012 period (Table 5).

Table 4. Annual sediment volume contribution (m^3/yr) by drift cell, 2001-2012.

Drift Cell	Mean (m^3/yr)	Mean + 1 S.D. (m^3/yr)	N (# transects)	Length (m)
Dungeness	103,000	232,000	433	13,625
Elwha	20,000	49,000	152	4,877

Table 5. Annual length-normalized sediment contribution (m^3/m/yr) by drift cell, 2001-2012.

Drift Cell	Mean (m^3/m/yr)	Mean + 1 S.D. (m^3/m/yr)	Max. (m^3/m/yr)	N (# transects)	Length (m)
Dungeness	7.5	17.0	11.3	433	13,625
Elwha	4.1	10.0	14.5	152	4,877

Short-term bluff change
Results from the boat-based LiDAR show bluff recession varies alongshore with higher rates of bluff recession in the Dungeness than the Elwha drift cell, and significantly more erosion of the bluff face overall between the second two surveys (March to August 2013) than was observed between the first two surveys (June 2012 to March 2013) (Figure 14). Within the Dungeness drift cell, there is a large-scale trend of higher rates to the east near Dungeness Spit and lower to the west near MacDonald Creek (Figure 14). Of the 104 profiles examined for the second two surveys (first two surveys), 7 (12) exhibited mean recession distances > 1 m and 21 (19) had maximum recession distances > 1 m (Figure 14). Continued monitoring is necessary for temporal variation due to infrequency of large-movement sediment events.

From June 2012 to August 2013, the mean recession distance for all of the profiles ranged from 0 m (no change or accretion measured) to 3.26 m, with a mean of 0.47 m (Figure 15A). The mean bluff recession rate for this stretch of shoreline between June 2012 and August 2013 is 0.41 m/yr (ranging from 0 to 2.79 m/yr (Figure 15B).

Between Dungeness Spit and MacDonald Creek, nine ground control targets were distinguishable in the LiDAR point cloud for the August 2013 survey (the georeferenced dataset to which the other two datasets were adjusted). The center point of each target from the point

cloud was compared to independently GPS-surveyed coordinates of the target, yielding a mean horizontal and vertical offset of 8 cm and 17 cm, respectively. This level of error corresponds well to an earlier calibration test survey we performed where we observed horizontal and vertical errors of 7 cm and 16 cm, respectively, when compared to a field of 21 targets at a range of ~35 m measured with a total station.

A)
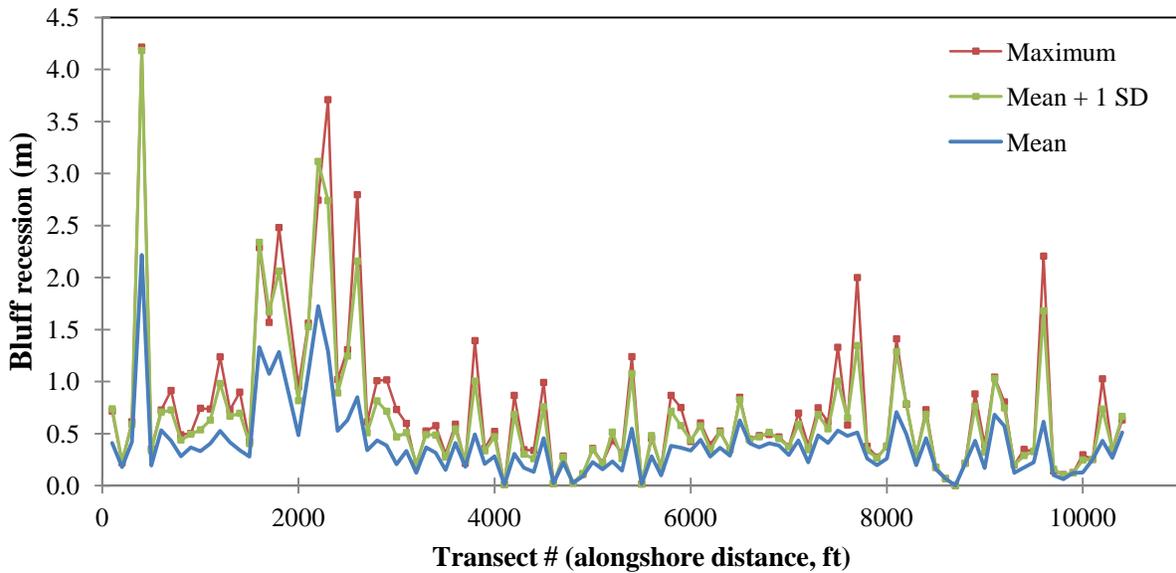
B)
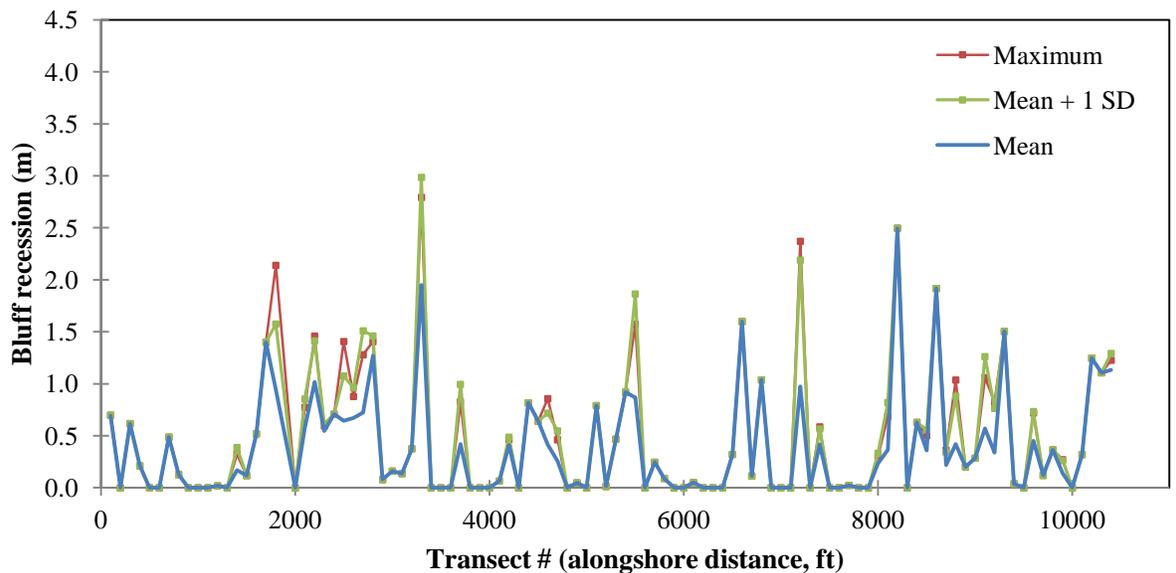
Figure 14. Alongshore distribution of bluff recession distance for transects 100-10400 along the Dungeness bluffs from (A) March to August 2013 and (B) June 2012 to March 2013.

A)

B)
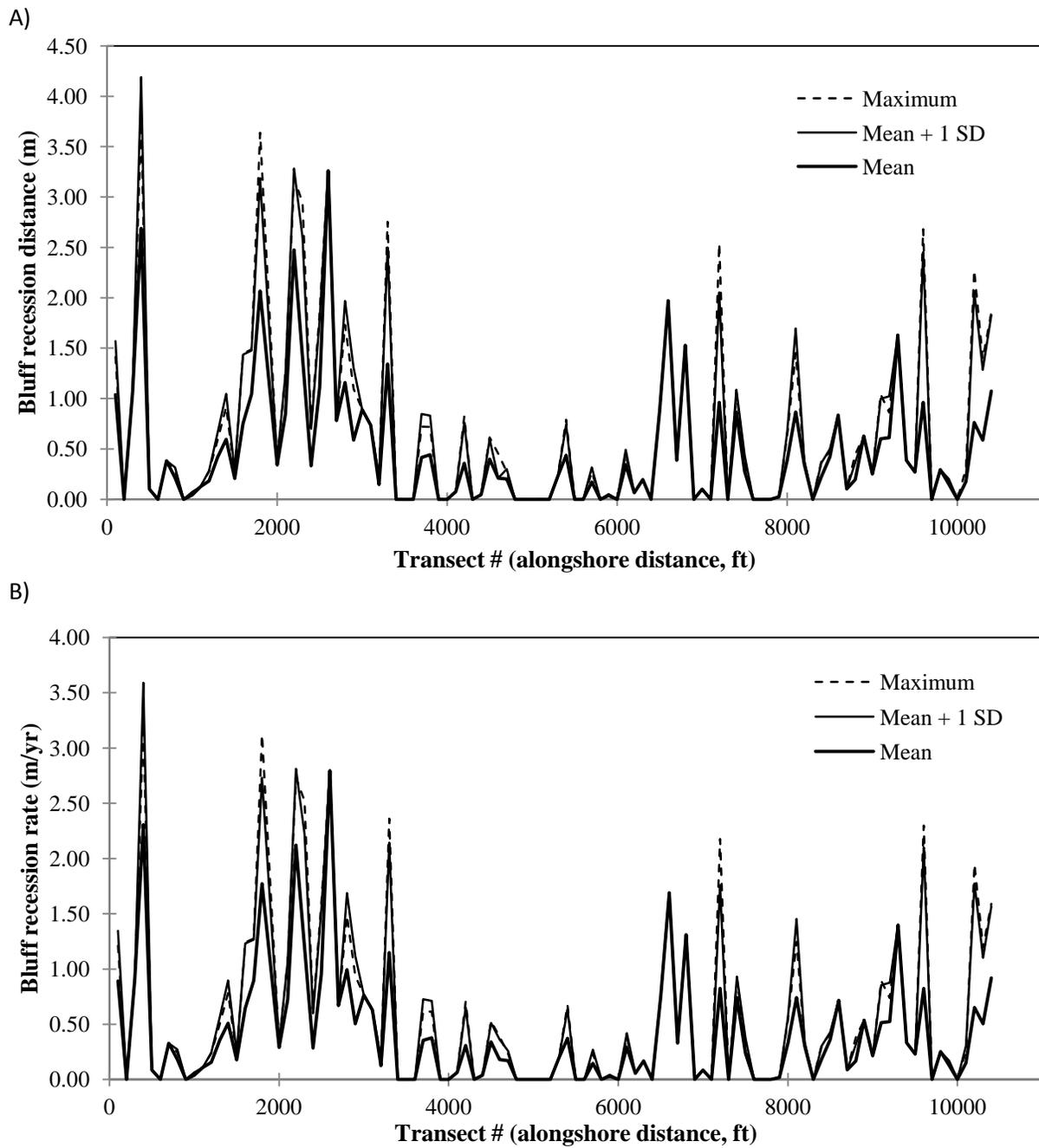
Figure 15. Alongshore distribution of (A) bluff recession distance and (B) associated rate for transects 100-10400 along the Dungeness bluffs between June 2012 and August 2013 derived from boat-based LiDAR.

Beach Sediment Volume Changes

Annual beach sediment volume changes as well as the net 3-year change at the twelve transect locations (eight along the Dungeness bluffs; four along the Elwha bluffs) are shown in Figure 15 and Tables 6 and 7. With the exception of transect EB-1 (where the effects of sediment supply from the Elwha River are evident), the general trend in beach sediment volume has been one of net loss over the three year period between 2010 and 2013.

In the Elwha drift cell, annual beach transect elevation changes ranged from -0.72 (net loss) to +1.19 m/yr (net gain) (mean = -0.13 ± 0.52 m/yr). The greatest loss at all Elwha transects was during 2010-2011. In the Dungeness drift cell, annual beach transect elevation changes ranged from -1.05 m/yr to +0.22 m/yr (mean = -0.19 ± 0.29 m/yr).
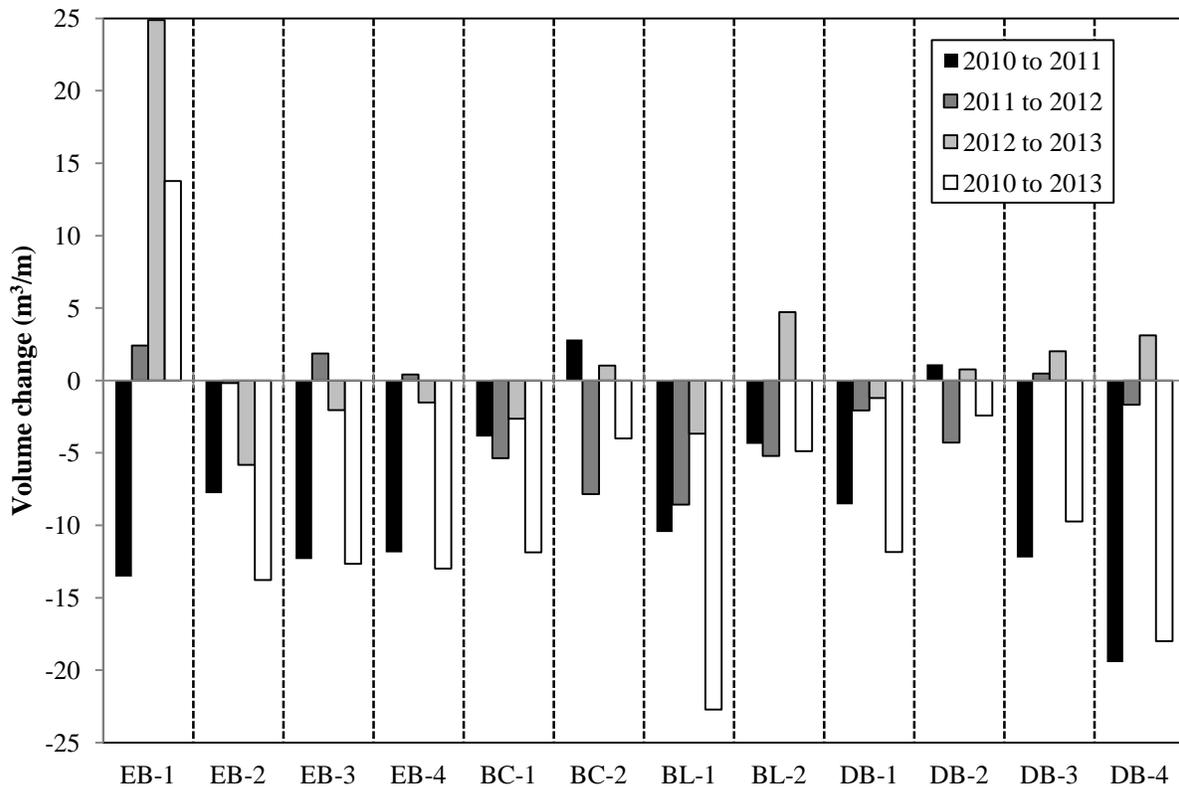
Figure 15. Length-normalized sediment volume change (m^3/m) in the highest 20 meters of each beach topographic profile during four winter-to-winter time intervals. EB-1 through BL-1 were winter surveys; BL-2 through DB-4 were summer surveys. Note that intervals 1-3 are annual whereas interval 4 spans 3 years.

Table 6. Beach topographic profile sediment volume changes for the Elwha drift cell. Note that the right-most column is net change between 2010-2013, while all others are annual intervals.

Profile	2010-2011		2011-2012		2012-2013		2010-2013	
	Volume Change (m^3/m)	Change Rate (m/yr)	Volume Change (m^3/m)	Change Rate (m/yr)	Volume Change (m^3/m)	Change Rate (m/yr)	Volume Change (m^3/m)	Change Rate (m/yr)
EB-1	-13.54	-0.69	2.42	0.12	24.89	1.19	13.77	0.23
EB-2	-7.77	-0.40	-0.17	-0.01	5.82	-0.28	-13.77	-0.23
EB-3	-12.33	-0.66	1.87	0.09	-2.06	-0.11	-12.66	-0.22
EB-4	-11.88	-0.72	0.41	0.02	-1.52	-0.08	-12.98	-0.23
Avg	-11.38	-0.62	1.13	0.06	3.87	0.18	-6.41	-0.11

Table 7. Beach topographic profile sediment volume changes for the Dungeness drift cell. Note that the right-most column is net change between 2010-2013, whereas all others are annual intervals.

Profile	2010-2011		2011-2012		2012-2013		2010-2013	
	Volume Change (m^3/m)	Change Rate (m/yr)	Volume Change (m^3/m)	Change Rate (m/yr)	Volume Change (m^3/m)	Change Rate (m/yr)	Volume Change (m^3/m)	Change Rate (m/yr)
BC-1	-3.87	-0.20	-5.37	-0.24	-2.63	-0.16	-11.86	-0.20
BC-2	2.83	0.15	-7.85	-0.34	1.02	0.06	-4.01	-0.07
BL-1	-10.47	-0.43	-8.57	-0.38	-3.67	-0.23	-22.72	-0.36
BL-2	-4.38	-0.22	-5.22	-0.29	4.73	0.20	-4.88	-0.08
DB-1	-8.56	-0.43	-2.07	-0.12	-1.22	-0.05	-11.84	-0.20
DB-2	1.11	0.06	-4.30	-0.24	0.76	0.03	-2.42	-0.04
DB-3	-12.23	-0.79	0.48	0.03	2.02	0.08	-9.73	-0.17
DB-4	-19.44	-1.05	-1.67	-0.09	3.10	0.14	-18.01	-0.31
Avg	-6.88	-0.36	-4.32	-0.21	0.51	0.01	-10.68	-0.18

Bluff Recession Model

Variables used for the simple bluff erosion model are shown in Table 8, with results shown in Figure 16. Ten future sea-level rise scenarios (factors of 1-10) are shown for the Dungeness and Elwha drift cells. The upper bound (sea-level rise approximately 9.7 mm/yr, factor 10) is equivalent to the estimated very high rate of sea-level rise published by Mote et al. (2008) for the Northwest Olympic Peninsula for the year 2050. The estimated potential increases in average bluff erosion rates range from 0-0.05 m/yr in the Elwha drift cell and 0-0.07 m/yr in the Dungeness drift cell (Figure 16).

Table 8: Variables used in the simple bluff recession model. Sc_1 (current sea1level rise) and S_{max} (upper hound of sea-level rise) from Mote et al. (2008). P from Parks et al. (2013). L and H are averaged over each respective drift cell.

Drift Cell	R_1	Sc_1 (m/yr)	S_{max} (m/yr)	L (m)	P	B_{max} (m)	H (m)	R_{max} (m/yr)
Dungeness	0.5	0.0016	0.016	353	0.95	80	7.8	0.5652
Elwha	0.4	0.0016	0.016	240	0.95	80	6	0.4452
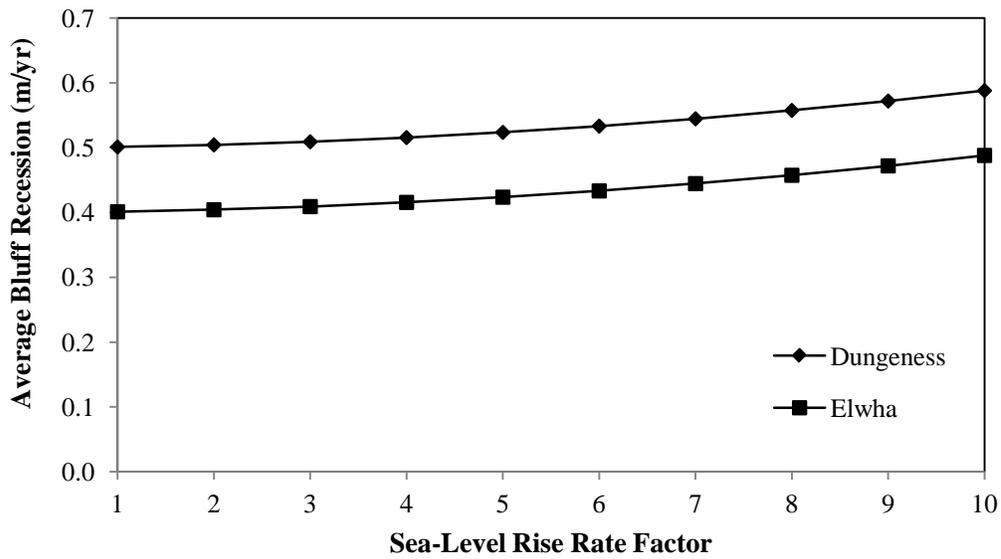
Figure 16. Average bluff recession rates as a factor of future sea-level rise rate (mm/yr) increases using the modified Bruun Rule equation from Lee (2005).

DISCUSSION

Bluff Recession Rates

Rates of bluff recession observed in this study in the Elwha drift cell generally agree with   rates measured by the U.S. Army Corps of Engineers (USACE, 1971) in the Elwha drift cell but are elevated over those observed by Keuler (1988) in the Dungeness drift cell and are substantially higher than the long-term rates observed by Rogers et al. (2012) for the Eastern Strait of Juan de Fuca shoreline. Rates of bluff recession observed between 2001 and 2012 may represent higher than average erosion rates due to high storm frequency and intensity occurring during this period: two time intervals, winters of 2007 and 2009, represent two of the wettest and windiest periods on record for this location (NCDC, 2014). Additionally, the 2001-2011 period experienced four high-tide events that exceeded the 50-year recurrence interval for extreme high water levels in the Central Strait of Juan de Fuca (NOAA, 2013).

Bluff recession rates observed in the Dungeness and Elwha drift cells in this study have immediate application to land-use planning for residential and commercial construction activities adjacent to the coastal bluffs. Given a typical design-life of a single family home of 100 years, applying the observed average bluff recession rates (Table 1) provides a minimum setback distance between a structure and the edge of the bluff of 42 m in the Elwha drift cell and 50 m in the Dungeness drift cell, based on average maximum long term rates. It should be noted that these rates of observed bluff recession fall closely in line with those published for the Elwha drift cell by Polenz et al. (2004) and represent the long-term post-glacial average bluff recession rate for the south shore of the Central Strait of Juan de Fuca.

Extending past observed bluff recession rates into the future is likely a simplistic and inaccurate method to determine future bluff recession (Hapke and Plant, 2010). Probabilistic methods of predicting bluff erosion (Lee et al., 2001; Walkden and Hall, 2005; Hapke and Plant, 2010) which accommodate spatial and temporal variability could be applied to the Dungeness and Elwha drift cells and would likely be more accurate than using hindcast observations of bluff recession. However, the data necessary to employ these procedures (e.g., wave and tidal height distributions along the bluffs) are not currently available.

Sediment Volume Change

Annual sediment volume contributions within the Elwha drift cell from this study (2.0×10^4 m^3/yr, Table 4) are consistent with the flux of 3.1×10^4 m^3/yr determined by USACE (1971). Furthermore, our calculated length-normalized rates of 4.1 m^3/m/yr (Elwha) and 7.5 m^3/m/yr (Dungeness) are consistent with a previous study by Keuler (1988) that measured sediment contribution rates for the exposed areas of the Strait of Juan de Fuca to range between 6-12 m^3/m/yr.

Sediment volume estimates for the Elwha drift cell from this study can inform the coastal sediment budget post-dam removal. Since shore-protection works in the Elwha drift cell will remain after the Elwha dams have been removed, a significant component of the Elwha drift cell

sediment budget will remain impaired after the sediment supply from the Elwha River has been restored.

Randle et al. (1996) estimates that the pre-dam fluvial sediment contribution to the Strait of Juan de Fuca was about 190,000 m^3/yr. In the Elwha drift cell, the current upper estimate of annual sediment volume contribution to the nearshore from bluff erosion is approximately 20,000-49,000 m^3/yr (Table 4) or about 11-26% of the pre-dam annual sediment contribution from the Elwha River. The current annual sediment volume contribution from bluff erosion in the Elwha drift cell represents a 90% reduction from the 1911 pre-armoring estimate (222,000 m^3/yr; USACE, 1971) but is roughly approximate to the 1960 post-armoring estimate (30,582 m^3/yr; Galster, 1989).

Comparing the sediment production rates between the Dungeness and Elwha bluffs demonstrates the level of impairment within the Elwha drift cell. When normalized for drift cell length, the Elwha bluffs produce 56% less sediment volume than the Dungeness bluffs on an annual basis. Comparing the measured rates of sediment production from bluffs (Table 5) vs. sediment volume change in beach transects (Tables 6 and 7, Figure 15) demonstrates the imbalance in the sediment supply relative to available sediment transport. In most years, the amount of available sediment volume contributed from bluffs to the beach is substantially less than the average rate of sediment loss leading to beach lowering and resulting in accelerated bluff erosion.

Airborne vs. Boat-Based LiDAR

Boat-based LiDAR enables efficient remote monitoring of coastal bluffs that are challenging to survey using traditional ground-based methods. Boat-based surveys can be quickly mobilized and provide a comparatively low-cost means to collect comprehensive, high-resolution topographic data on a project scale. Though one of the challenges faced with boat-based LiDAR is that it is difficult to obtain returns on the ground surface of densely vegetated areas, it is the ideal method for measuring coastal bluff erosion. The near-horizontal look angle of the laser allows for high coverage and accuracy on high-relief shoreline topography and vertical features, such as bluffs and shoreline armoring, as well as collecting data under overhanging structures or vegetation.

The data density across the beach and adjacent uplands is significantly greater than the resolution typically obtained by airborne LiDAR (20-40 points/m^2 vs. 8 points/m^2). This density difference enables boat-based LiDAR to detect smaller changes in the bluff face and therefore makes it more suitable for quantifying bluff erosion and sediment supply on shorter time scales or along coasts such as Puget Sound where chronic erosion rates are generally small and may go undetected by airborne LiDAR. In particular, along pocket beaches and short drift cells with beaches dependent upon bluff erosion as the source of sediment, relatively small volumes may be critical to maintaining the beach sediment budget and associated physical and ecological attributes of the nearshore.

Moreover, with airborne LiDAR, the back beach and key features such as the bluff crest or toe are typically blurred due to resolution of the dataset. During the DEM gridding process, a grid

cell may be attributed with a weighted average value of all LiDAR returns that fall within the grid cell. If, for example, 50% of those LiDAR returns come from the top of the bluff and 50% come from the steep bluff face immediately seaward, the grid cell value will have a lower elevation than if the grid cell was 100% populated with bluff-top elevations and the adjacent grid cell seaward were 100% populated with bluff-face elevations. Because of this, the bluff top may appear lower and more rounded than it is in reality (Figure 17), skewing estimates of bluff recession and volume change.
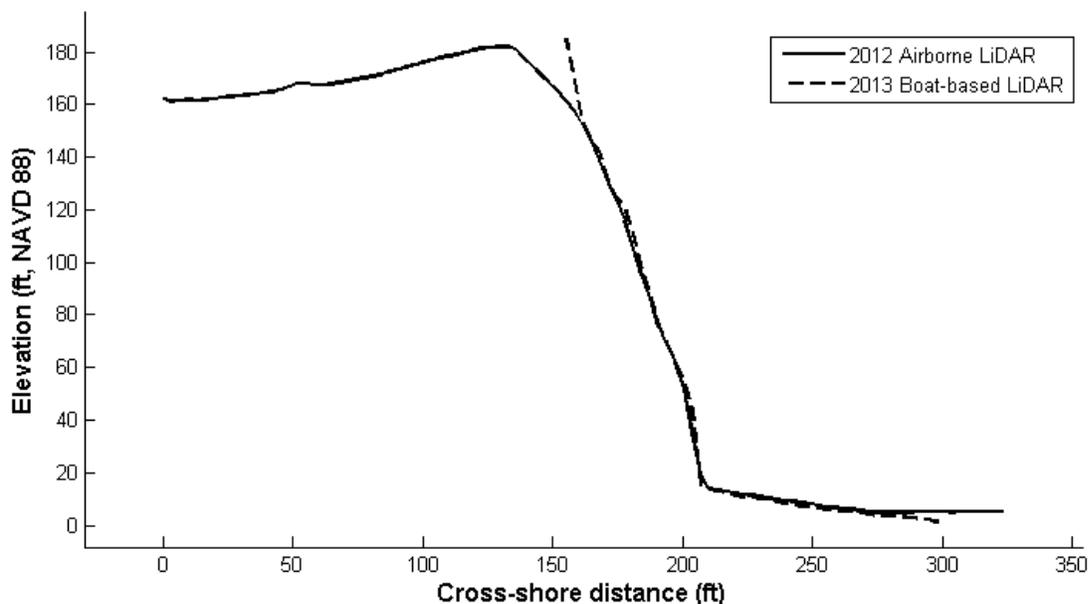
Figure 17. Cross-shore profile of bluff face illustrating how bluff crest can be obscured in an airborne LiDAR DEM when compared to a DEM generated from boat-based LiDAR data that is more optimal for vertical surfaces.

Boat-based LiDAR Challenges, Successes, and Uncertainty

Three boat-based LiDAR surveys were performed over 1.2 years as an effort to monitor the coastal bluffs of the Elwha and Dungeness drift cells in Clallam County, Washington. The data collected during the surveys was used to build bare earth DEMs from which we could calculate beach and bluff change between the surveys through profile analysis as well as difference surfaces. The results of analysis of the three subsequent surveys presented here are based on vector adjustments to align scans, but more work remains in the collaboration with hardware and software developers to isolate and resolve highly detailed georeferencing and data transformation issues.

With the time and resource constraints of a single project of approximately two years, it is challenging to initiate cutting-edge sophisticated technology, establish associated data collection and processing methodologies, and at the same time provide data deliverables that can be readily integrated with land-use planning and coastal management. Establishing a fully calibrated

system, complete with field verification of data and error analysis, remains as a work in progress. Nevertheless, the key objectives and deliverables of the project were accomplished, the technology has been proven, and the capacity now exists to provide decision-makers with advanced information and tools with regard to bluff erosion processes for improved management of bluff-top development and land use. With only a little over a year of data, bluff face change analysis provided new insights to chronic and event-based mechanisms and processes of bluff erosion as well as bluff recession rates and volume changes to put in context with longer term results derived from aerial photos and airborne LiDAR.

Simultaneously-acquired photographs and resulting photomosaics complement the boat-based LiDAR data for visualization and interpretation during processing. Methods were developed in this project to enable direct overlay of georeferenced photos onto LiDAR DEMs to aid in data processing, quality control, and classification point clouds. To qualitatively ground-truth the difference surface results, the digital photos collected during each survey were examined for evidence of volume change through time. An example of this is illustrated by the photos in Figure 18, which are of the same area that is shown by the difference surfaces in Figure 19. When comparing the photos from June 2012 to March 2013 (Figures 18A and 18B), it is difficult to assess whether any change has occurred in the circled area and the difference surface shows insignificant change either (Figure 19A). However, between March 2013 and August 2013 (Figures 18B and 18C), the photos clearly show that the scour on the bluff face has deepened and appears to have grown in length, moving closer to the top of the bluff. These observations are concurrent with what is shown in the difference surface between these two surveys (Figure 19B).

Among the accomplishments not central to the project, yet applicable in continuing efforts, is the feasibility of classifying features in the LiDAR point cloud such as vegetation, talus deposits, woody debris (LWD), and shoreline armoring, and extracting associated quantities to better characterize their relationship to bluff sediment supply. Of particular relevance to the project objectives was finding a correspondence of shoreline armoring to significantly lower bluff erosion rates with only three surveys performed over 14 months. The results suggest that armoring of beaches below feeder bluffs restricts sediment supply into the littoral drift system.

As discussed in the results, for this survey, we have measured an average horizontal and vertical offset of 8 cm and 17 cm, respectively, of the point cloud to the independently surveyed target positions. Manufacturer specifications for the laser scanner state a raw range accuracy of 7 mm at 100 m (Optech, 2014). The POS MV 320 is capable of positional accuracies of 0.5-2 m with DGPS and 8 mm in the horizontal, 15 mm in the vertical with RTK. Heading errors are on the order of 0.02°, while expected roll and pitch errors are 0.008° (after post-processing in POSPac MMS). Sources of error are numerous and difficult to quantify, including accuracy of the laser scanner, accuracy of the IMU, accuracy of the R8 rover, the ability to measure the center of the target in the field, accuracy of the lever arm measurements (sensor locations relative to the vessel reference point), accuracy of the boresight parameters (pitch, roll, and heading offsets for the laser scanner), accuracy of the base station locations used in post-processing, and the ability to pick the center of the target in the point cloud.

Figure 18. Digital photos taken during each of the three boat-based LiDAR surveys; used to qualitatively verify the results of the difference surfaces shown in Figure 19.
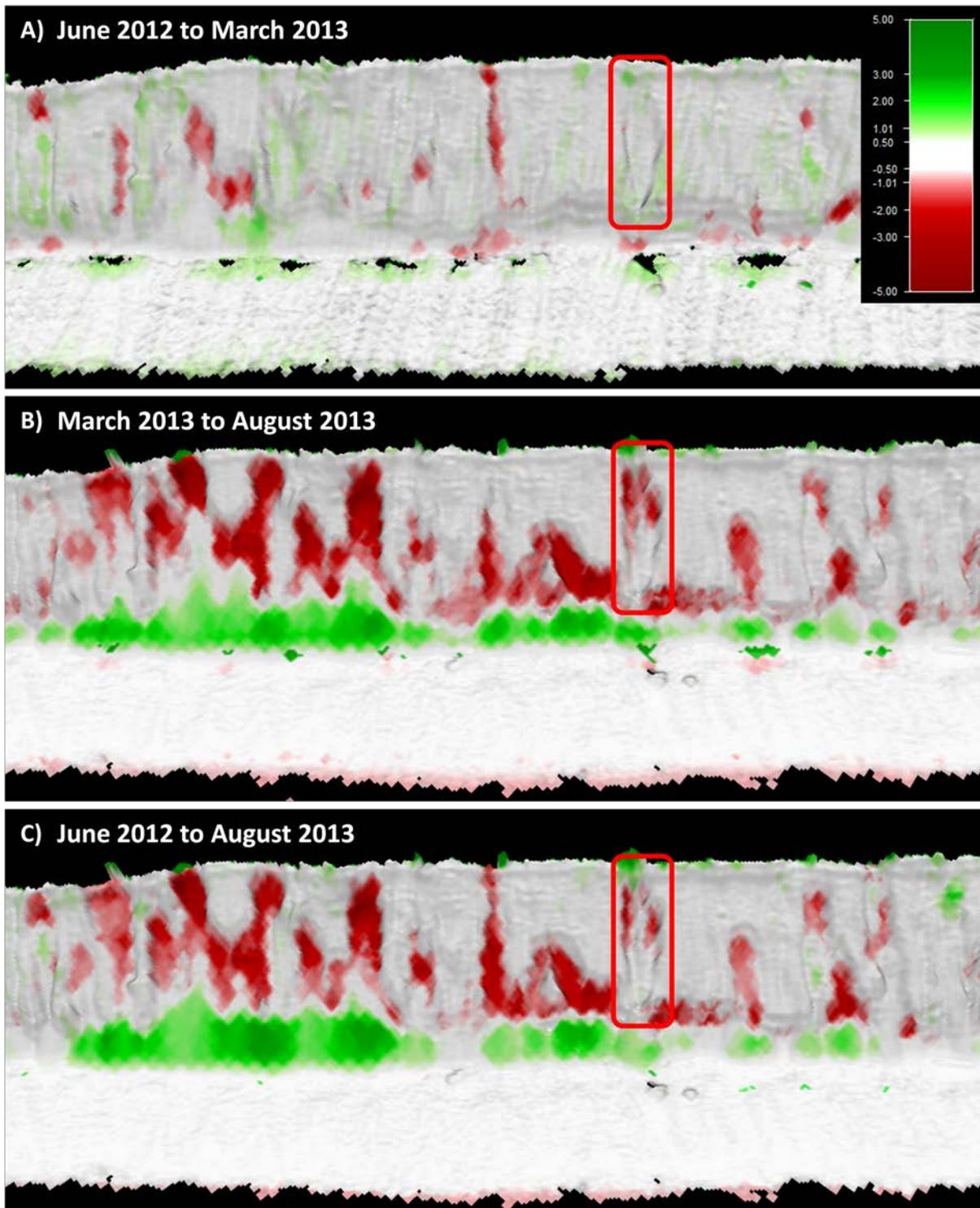
Figure 19. Difference surfaces illustrating the amount of erosion (red) or accretion (green) that has occurred for a section of the Dungeness bluffs as measured from the three boat-based LiDAR surveys conducted between June 2012 and August 2013.

Bluff Erosion Model

Sea-level rise and climate change pose unique challenges to coastal bluffs, especially when they are the sole source of sediment to adjacent beaches, barriers, and their associated nearshore habitats. Many factors, including wave impacts, high water levels, upland land-use patterns, precipitation, ground-water saturation, and geology influence bluff erosion. Conceptual models describing the processes linking these factors to bluff erosion are compelling but there are few quantitative studies to support them. Additionally, climate change is expected to accelerate sea-level rise, increase storm intensity and frequency, and increase precipitation intensity, and will therefore likely accelerate bluff erosion.

While this project obtained high resolution data to enhance the understanding of bluff erosion processes, complementary data needed to link erosion patterns to wave energy, water levels, and precipitation patterns were beyond the scope of effort needed to develop forecasts of bluff erosion under several climate change scenarios. Thus a simplistic model was applied to demonstrate the effect of sea-level rise on bluff erosion in the future.

Until specific studies are undertaken to capture event forcing and bluff response, only anecdotal observations can be made to speculate on the relative importance of the factors governing bluff erosion. At present the best use of available data is to extrapolate long term bluff recession rates in context with accelerated erosion based on projected sea-level rise scenarios and short-term event-based erosion magnitudes as discussed further below.

Management Implications

One of the key outcomes of this project was that boat-based LiDAR obtained sub-meter resolution data at very high density along the bluffs that is much more robust than the previous airborne LiDAR data sets. At the same time, producing a sediment budget and bluff erosion rates needed for management purposes require longer term datasets such as from aerial photos and airborne LiDAR presented in this paper. This limits the ability to fully benefit from this new mapping technique until additional boat-based LiDAR data are collected in the future.

To approach medium-term bluff recession rates to the extent possible, the third boat-based LiDAR survey collected in August 2013 was analyzed for change with respect to the 2012 airborne LiDAR DEM. These rates were then compared to those obtained from the 2001-2012 airborne LiDAR data and put into further context of the short term observations obtained from the inter-comparisons of the three boat-based LiDAR datasets.

Bluff recession rates were shown to vary depending on the time of measurement and length of observation. While the short-term change observations from the boat-based LiDAR reveal important bluff erosion patterns, it is not appropriate to extrapolate short-term measurements into long-term rates, especially if the length of measurement is less than the time span of the rate being reported (e.g., producing an annual rate from < 1 year of observation). For instance, a measurement taken over a month when there was a large bluff failure could result in huge overestimates of bluff recession on an annual basis if there was no further change for the

remainder of the year. Moreover, using the maximum measured recession distance to calculate an annual recession rate will result in an even greater overestimate and could give a false impression of how much the bluff is actually retreating. The maximum recession distance is measured for a specific point along the bluff and may not represent the trends observed over the larger area. It would be more correct to calculate a mean bluff recession distance for a given area measured over a long period of time (i.e., years to decades). The long-term rates should then be qualified with the amount of recession that may occur during a given event (e.g., the average maximum recession distance). As an example, for land-use management, it would be more appropriate to use a long-term mean recession rate over the horizon of interest to obtain a setback distance with an added buffer based on event-scale recession.

It should be emphasized that bluff recession distances reported in this report are derived from selected elevations across the bluff-face profile which may not be seen by the homeowner at the bluff top. While the trends are not likely to significantly change, results will differ according the methods used to analyze bluff-face change. Other methods of calculating bluff recession distances (e.g., contour change analysis, volume change analysis) are expected to provide different results than the profile-based methods used herein, and the potential to produce alongshore averaging of bluff recession rates over appropriate alongshore length scales may result in less spatially variable rates that are more conducive to land-use zoning, buffers, and development setbacks. The bluff-face profile method has the potential to accentuate the localized erosion signals due to a lack of continuity along the bluff to enable alongshore averaging commensurate with the observed signals of change obtained at finer scale along the bluff face.

While land-use planners and coastal managers are in need of long-term erosion rates for prudent resource management, property owners experience localized erosion and tend to be most interested and concerned about the magnitude of bluff recession occurring along relatively small increments of space along their bluff-top property boundary. Thus, a key advantage of boat-based LiDAR data is the ability to deliver high-resolution spatially explicit data products that reveal detailed topographic relief and depictions of bluff recession over relevant time scales to highly localized parcel-by-parcel decision-making. This ability enables property owners and coastal managers alike to take a more refined approach in grappling with bluff erosion impacts as well as the consequences of attempting to mitigate bluff erosion.

CONCLUSIONS

Rates of coastal bluff recession in the Dungeness and Elwha drift cells over the 1939-2013 period were highly variable in space and time and ranged between 0.31 m/yr and 3.25 m/yr. Differences between maximum near term bluff erosion rates observed from 2013 boat-based LiDAR and longer term (1939-2001) observations from digitized historical photography were the result of individual medium-scale landslides. The presence of shoreline armoring is a controlling factor on the rate of bluff recession with armored bluffs showing a reduced recession rate compared with unarmored bluffs. The volume of sediment produced by a unit length of unarmored bluff shoreline is greater than armored bluffs by a factor of two (Elwha) and five (Dungeness).

While wave run-up and erosion at the base of coastal bluffs is a dominant driving factor of erosion throughout both drift cells, portions of each drift cell also showed that erosion was occurring in the upper third of the bluff profile and was driven by precipitation and local groundwater discharge. Upper bluff erosion driven by groundwater and precipitation is not influenced by shoreline processes and protection works and will continue whether the shoreline is armored or not.

Analysis with a simple bluff erosion model using the modified Bruun Rule equation suggests that future potential rates of sea level rise in the Strait of Juan de Fuca have the potential for increasing bluff erosion rates by up to 0.1 m/yr by the year 2050.

At present, it remains challenging to make reliable projections of bluff recession that may guide development setback distances for the future, given the coarse-resolution of a multi-decadal interval (aerial photos for 1939-2001), only one higher-resolution decadal interval (airborne LiDAR data for 2001-2012) and the short term event-scale observations of fairly localized erosion events. The combination of chronic recession rates and event-based erosion magnitudes are important for decision-makers, and the most reliable rates will come from a longer term high-resolution dataset that must be developed over time.

The resolution of bluff-face change obtainable with boat-based LiDAR presents the possibility to greatly enhance the understanding of bluff erosion processes. For example, repeat surveys performed at relatively short intervals would enable a better determination of the relative importance of a variety of mechanisms contributing to bluff erosion such as surface runoff (and associated land clearing and development practices), wind, precipitation, groundwater discharge, soil saturation, wave height and direction, total water level, beach elevation, and littoral sediment supply. All of these factors play a role in bluff retreat dynamics and measurement of these parameters combined with high-resolution bluff-face topography and differences over time will enable improved process-based bluff erosion models.

ACKNOWLEDGEMENTS

REFERENCES

Alho, P.; Kukko, A.; Hyyppa, H.; Kaartinen, H.; Hyyppa, J.; and Jaakkola, A., 2009, Application of boat-based laser scanning for river survey: *Earth Surface Processes and Landforms*, Vol. 34, pp. 1831-1838.

Applanix, 2013, POS MV 320 Specifications, available at: http://www.applanix.com/media/downloads/products/specs/posmv320_specifications.pdf

Booth, D. B.; Troost, K. G.; Clague, J. J.; and Waitt, R. B., 2003, The cordilleran ice sheet: *Development in Quaternary Science*, Vol. 1, pp. 17-43.

Bountry, J. A.; Ferrari, R.; Wille, K.; and Randle, T. J., 2010, *2010 Survey Report and area-capacity tables for Lake Mills and Lake Aldwell on the Elwha River, Washington*: Denver, CO, U.S. Department of Interior, Bureau of Reclamation, Technical Service Center, Report No. SRH-2010-23, 66 p.

Bikfalvi, 2012, ABOXPLOT, advanced boxplot routine for MATLAB, available at: http://alex.bikfalvi.com/research/advanced_matlab_boxplot/

Bradley, W. C., 1963, Large-scale exfoliation in massive sandstones of the Colorado Plateau: *Geological Society of America Bulletin*, Vol. 74, pp. 519-528.

Bray, M. J. and Hooke, J. M., 1997, Prediction of soft-cliff retreat with accelerating sea-level rise: *Journal of Coastal Research*, Vol. 13, No. 2, pp. 453-467.

Buckley, S. J.; Howell, J. A.; Enge, H. D.; and Kurz, T. H., 2008, Terrestrial laser scanning in geology: data acquisition, processing and accuracy considerations: *Journal of the Geological Society*, London, Vol. 165, No. 3, pp. 625-638.

Carson, M. A. and Kirkby, M. J., 1972, *Hillslope Form and Processes*: Cambridge University Press, Cambridge, 475 p.

Collins, B. D. and Sitar, N., 2005, Monitoring of Coastal Bluff Stability Using High Resolution 3D Laser Scanning: *ASCE Conference Proceedings*, Vol. 164, No. 5.

Collins, B. D. and Sitar, N., 2008, Processes of coastal bluff erosion in weakly lithified sands, Pacifica, California, USA: *Geomorphology*, Vol. 97, No. 3-4, pp. 483-501.

Dean, R. G., 1991, Equilibrium beach profiles: characteristics and applications: *Journal of Coastal Research*, Vol. 7, No. 1, pp. 53-84.

Dethier, D. P.; Pessl, Jr., F.; Keuler, R. F.; Balzarini, M. A.; Pevear, D. R., 1995, Late Wisconsinan glaciomarine deposition and isostatic rebound, northern Puget Lowland, Washington: *Geological Society America Bulletin,* Vol. 107, No. 11, pp. 1288–1303.

Downing, J., 1983, *The coast of Puget Sound: it's processes and development*: University of Washington Press, Seattle, WA, 126 p.

Drost, B. W., 1986, *Water Resources of Clallam County, Washington*: U.S. Geological Survey Water Resources Investigations Report 83-4227.

Finlayson D. P., 2005, *Combined bathymetry and topography of the Puget Lowland, Washington State*: University of Washington, Seattle, WA, available at: http://www.ocean.washington.edu/data/pugetsound/

Finlayson, D., 2006, *The Geomorphology of Puget Sound Beaches*: Puget Sound Nearshore Partnership Report No. 2006-02, Washington Sea Grant Program, University of Washington, Seattle, WA.

Galster, R. W., 1989, Ediz Hook - acase history of coastal erosion and mitigation. Engineering Geology in Washington, Volume II: *Washington Division of Geology and Earth Resources Bulletin* 78, Washington Department of Natural Resources, Olympia, WA, pp. 1177-1186.

Galster, R. W. and Schwartz, M. L., 1989, Ediz Hook—A case history of coastal erosion and rehabilitation. In Schwartz, M. L. and Bird, E. C. F. (Editors), *Artificial Beaches, Journal Coastal Research*, Special Issue 6.

Gelfenbaum, G.; Stevens, A.; Elias, E.; and Warrick, J., 2009, Modeling sediment transport and delta morphology on the dammed Elwha River, Washington State, USA: *Coastal Dynamics* 2009, Paper No. 109.

Gelfenbaum, G.; Stevens, A. W.; Miller, I. M.; Warrick, J. A.; Ogston, A. S.; and Eidam, E., In Review, Large-scale dam removal on the Elwha River, Washington, USA: Coastal Geomorphic Change: Submitted to *Geomorphology*.

Gilbert, J. and Link, R. A., 1995, *Alluvium distribution in Lake Mills, Glines Canyon Project and Lake Aldwell, Elwha Project, Washington*: U.S. Department of Interior, Elwha Technical Series PN-95-4, 60 p.

Hampton, M. A., 2002, Gravitational failure of sea cliffs in weakly lithified sediment: *Environmental and Engineering Geoscience*, Vol. VIII, No. 3, pp. 175-191.

Hapke, C., 2004, The measurement and interpretation of coastal cliff and bluff retreat. *In* Hampton, M. and Griggs, G. (Editors), *Formation, evolution, and stability of coastal cliffs – Status and trends*. U.S. Geological Survey Professional Paper 1693, pp. 39-50.

Hapke, C. J. and Plant, N., 2010, Predicting coastal cliff erosion using a Bayesian probabilistic model: *Marine Geology*, Vol. 278, pp. 140-149.

Johannessen, J. and MacLennan, A., 2007, *Beaches and Bluffs of Puget Sound*: Puget Sound Nearshore Partnership Report No. 2007-04, Seattle District, U.S. Army Corps of Engineers, Seattle, WA.

Jones, M. A., 1996, *Delineation of Hydrogeologic Units in the Lower Dungeness River Basin, Clallam County, Washington*: U.S. Geological Survey, Water Resources Investigation Report 95-4008.

Keuler, R. F., 1988, *Map showing coastal erosion, sediment supply, and longshore transport in the Port Townsend 30-by-60-minute quadrangle, Puget Sound region, Washington*: U.S. Geologic Survey Miscellaneous Investigation Map I-1198-E, scale 1:100,000.

Kraus, N. C.; Larson, M.; and Wise, R. A., 1998, *Depth of Closure in Beach-fill Design*: Coastal Engineering Technical Note CETN II-40, U.S. Army Engineer Waterways Experiment Station, Vicksburg, MS.

Lee, E. M., 2005, Coastal cliff recession risk: a simple judgment-based model: *Quarterly Journal of Engineering Geology and Hydrogeology*, Vol. 38, pp. 89-104.

Lee, E. M.; Hall, J. W.; and Meadowcroft, I. C., 2001, Coastal cliff recession: the use of probabilistic prediction methods: *Geomorphology,* Vol. 40, pp. 253-269.

Miller, I. M.; Warrick, J. A.; and Morgan, C., 2011, Observations of coarse sediment movements on the mixed beach of the Elwha Delta, Washington: *Marine Geology*, Vol. 282, No. 3-4, pp. 201-214.

Mosher, D. C. and Hewitt, A. T., 2004, Late Quaternary deglaciation and sea-level history of eastern Juan de Fuca Strait, Cascadia: *Quaternary International*, Vol. 121, pp. 23-39.

Mote, P.; Petersen, A.; Reeder, S.; Shipman, H.; and Binder, L. W., 2008, *Sea Level Rise in the Coastal Waters of Washington State*: University of Washington, Climate Impacts Group and the Washington Department of Ecology.

National Oceanic and Atmosperic Administration (NOAA), 2013, *Tidal data for Port Angeles, Washington, Station 9444090*, available at http://tidesandcurrents.noaa.gov/stationhome.html?id=9444090

National Climate Data Center (NCDC), 2014, Climate Summaries for Port Angeles and Sequim, Washington.

Olsen, M. J.; Johnstone, E.; Ashford, S. A.; Driscoll, N.; Young, A. P.; Hsieh, T.J.; and Kuester, F., 2008, Rapid Response to Seacliff Erosion in San Diego County using Terrestrial LIDAR: *Proceedings Solutions to Coastal Disasters Conference*, ASCE, Oahu, Hawaii, pp. 573-583.

Olsen, M. J.; Johnstone, E.; Driscoll, N.; Ashford, S. A.; and Kuester, F., 2009, Terrestrial laser scanning of extended cliff sections in dynamic environments: parameter analysis: *ASCE*

Journal of Surveying Engineering, Vol. 135, No. 4, pp. 161-169.

Optech, Inc., 2014, ILRIS Summary Specification Sheet, available at:
http://www.optech.com/wp-content/uploads/specification_ilris.pdf

Parks, D.; Shaffer, A.; and Barry, D., 2013, Nearshore drift-cell sediment processes and
ecological function for forage fish: implications for ecological restoration of impaired
Pacific Northwest marine ecosystems, *Journal of Coastal Research*, Vol. 29, No. 4, pp. 984-
997.

Polenz, M.; Wegmann, K.W.; and Schasse, H.W., 2004, *Geologic map of the Elwha and Angeles
Point 7.5-minute Quadrangles, Clallam County, Washington*: Washington Division of
Geology and Earth Resources, Open File Report 2004-14.

Puget Sound LiDAR Consortium (PSLC), 2001, Topographic LiDAR: Clallam County, WA.

Quan, S.; Kvitek, R.; Smith, D.; and Griggs, G., 2013, Using vessel-based LIDAR to quantify
coastal erosion during El Niño and inter-El Niño periods in Monterey Bay, California:
Journal of Coastal Research, Vol. 29, No. 3, pp. 555-565.

Randle, T. J.; Young, C. A.; Melena, J. T.; Ouellette, E. M., 1996, *Sediment analysis and
modeling of the river erosion alternative*: U.S. Bureau of Reclamation, Pacific Northwest
Region, Elwha Technical Series PN-95-9, 138 pp.

Rice, C. A., 2006, Effects of shoreline modification on a northern Puget Sound Beach:
microclimate and embryo mortality in surf smelt (*Hypomesus pretiosus*): *Estuaries and
Coasts*, Vol. 29, No. 1, pp. 63-71,

Rogers, H. E.; Swanson, T. W.; and Stone, J. O., 2012, Long-term shoreline retreat rates on
Whidbey Island, Washington, USA: *Quarternary Research*, oi:10.1016/j.yqres.2012.06.001.
University of Washington, Published by Elsevier Inc.

Schasse, H. W., 2003, *Geologic Map of the Washington Portion of the Port Angeles 1:100,000
quadrangle*: Washington Division of Geology and Earth Resources, Open File Report 2003-
6, Washington Department of Natural Resources, Olympia, WA.

Schasse, H. W. and Polenz, M., 2002, *Geologic Map of the Morse Creek 7.5-Minute
Quadrangle, Clallam County, Washington*: Washington Division of Geology and Earth
Resources, Open File Report 2002-8, Washington Department of Natural Resources,
Olympia, WA.

Schasse, H. W.; Polenz, M.; and Wegmann, K. W., 2000, *Geologic Map of the Carlsborg 7.5-
Minute Quadrangle, Clallam County, Washington*: Washington Division of Geology and
Earth Resources, Open File Report 2000-7, Washington Department of Natural Resources,
Olympia, WA.

Schuenemeyer, J. H. and L. J. Drew, 2011, *Statistics for Earth and Environmental Scientists*: John Wiley & Sons, Inc., Hoboken, NJ.

Schwartz, M. L.; Fabbri, P.; and Wallace, R. S., 1987, Geomorphology of Dungeness Spit, Washington, USA: *Journal of Coastal Research*, Vol. 3, No. 4, pp. 451-455.

Schwartz, M. L.; Wallace, R. S.; and Jacobsen, E. E., 1989, Net shore-drift in Puget Sound, Engineering Geology in Washington, Volume II, Olympia, WA: *Washington Division of Geology and Earth Resources Bulletin 78*, Washington Department of Natural Resources, pp. 1137-1146.

Shaffer, J. A.; Crain, P.; Kassler, T.; Penttila, D.; and Barry, D., 2012, Geomorphic habitat type, drift cell, forage fish and juvenile salmon; are they linked? *Journal of Environmental Science and Engineering*, Vol. 1, No. 5a, pp. 2162-5298.

Shipman, H., 2004, Coastal bluffs and sea cliffs on Puget Sound, Washington, In *Formation, evolution and stability of coastal cliffs-status and trends*: U.S. Geological Survey Professional paper 1693, 123 p.

Shipman, H.; Dethier, M. N.; Gelfenbaum, G.; Fresh, K. L.; and Dinicola, R. S. (Editors), 2010, Puget Sound shorelines and the impacts of armoring: Proceedings of the State of the Science Workshop, May 2009, Menlo Park, CA: U.S. Geological Survey Scientific Investigations Report 2010-5254, 262 p.

Stewart, J. P.; Hu, J.; Kayen, R. E.; Lembo, A. J.; Collins, B. D.; Davis, C. A.; and O'Rourke, T. D., 2009, Use of Airborne and Terrestrial Lidar to Detect Ground Displacement Hazards to Water Systems, *Journal of Survey Engineering*: Vol. 135, No. 3, pp. 119-124.

Stevens, A. W., 2014, personal communication, U.S. Geological Survey, Pacific Coastal and Marine Science Center, 400 Natural Bridges Dr, Santa Cruz, CA 95060.

Storlazzi, C. D.; Barnard, P. L.; Collins, B. D.; Finlayson, D. P.; Golden, N. E.; Hatcher, G. A.; Kayen, R. E.; and Ruggiero, P., 2007, *High-resolution topographic, bathymetric, and oceanographic data for the Pleasure Point area, Santa Cruz County, California; 2005-2007*: U.S. Geological Survey Open-File Report 2007–1270.

U.S. Army Corps of Engineers (USACE), 1971, *Report on Survey of Ediz Hook For Beach Erosion and Related Purposes. Port Angeles, Washington*: Department of the Army, Seattle District, Corps of Engineers, 96 p.

U.S. Geological Survey (USGS), 2012, U.S. Geological Survey Earth Resources Observation and Science Center, Sioux Falls, SD.

Varnes, D. J., 1978, Slope movement types and processes, In Clark, M. (Editor), *Landslide Analysis and Control*, Special Report 176, Transportation Research Board, National Academy of Sciences, National Research Council, Washington, DC, pp. 11-33.

Walkden, M. J. A. and Hall, J. W., 2005, A predictive Mesoscale model of the erosion and profile development of soft rock shores: *Coastal Engineering*, Vol. 52, pp. 535-563.

Warrick, J. A.; George, D. A.; Gelfenbaum, G.; Ruggiero, P.; Kaminsky, G. M.; and Beirne, M., 2009, Beach morphology and change along the mixed grain-size delta of the dammed Elwha River, Washington: *Geomorphology*, Vol. 111, pp. 136-148.

Yotter-Brown, C. W. and Faux, R., 2012, LiDAR remote sensing, Jefferson and Clallam Counties, Washington: *Puget Sound LiDAR Consortium*, Seattle, WA, 29 p.

Young, A. P. and Ashford, S. A., 2007, Quantifying sub-regional seacliff erosion using mobile terrestrial LIDAR, *Shore and Beach*, Vol. 75, No. 3, 38-43.

Young, A. P.; Olsen, M. J.; Driscoll, N.; Gutierrez, R.; Guza, R. T.; Flick, R. E.; Johnstone, E.; and Kuester, F., 2009, Comparison of Airborne and Terrestrial Lidar Estimates of Seacliff Erosion in Southern California, *Photogrammetric Engineering and Remote Sensing*, Vol. 76, No. 4, pp. 421-426.

Young, A. P.; Raymond, J. H.; Sorenson, J.; Johnstone, E. A.; Driscoll, N. W.; Flick, R. E.; and Guza, R. T., 2010, Coarse sediment yields from seacliff erosion in the Oceanside Littoral Cell: *Journal of Coastal Research*, Vol. 26, No. 3, pp. 580-585.

Young, A. P.; Guza, R. T.; O'Reilly, W. C.; Flick, R. E.; and Gutierrez, R., 2011, Short-term retreat statistics of a slowly eroding coastal cliff: *Natural Hazards and Earth System Sciences*, Vol. 11, pp.205-217.

Zilkoski, D. B.; Richards, J. H.; and Young, G. M., 1992, Results of the general adjustment of the North American vertical datum of 1988, (NAVD 88): *American Congress on Surveying and Mapping*, Surveying and Land Information Systems, Vol. 52, No. 3, pp. 133-149.